

A Unified Complexity-Algorithm Account of Constant-Round QAOA Expectation Computation

Jingheng Wang^{1,2}, Shengminjie Chen^{1,2}, Xiaoming Sun^{1,2}, and Jialin Zhang^{1,2}

¹State Key Lab of Processors, Institute of Computing Technology, Chinese Academy of Sciences, 100190, Beijing, China.

²School of Computer Science and Technology, University of Chinese Academy of Sciences, Beijing, 100049, China.

The Quantum Approximate Optimization Algorithm (QAOA) is widely studied for combinatorial optimization and has achieved significant advances both in theoretical guarantees and practical performance, yet for general combinatorial optimization problems the expected performance and classical simulability of fixed-round QAOA remain unclear. Focusing on Max-Cut, we first show that for general graphs and any fixed round $p \geq 2$, exactly evaluating the expectation of fixed-round QAOA at prescribed angles is NP-hard, and that approximating this expectation within additive error $2^{-O(n)}$ in the number n of vertices is already NP-hard. To evaluate the expected performance of QAOA, we propose a dynamic programming algorithm leveraging tree decomposition. As a byproduct, when the p -local treewidth grows at most logarithmically with the number of vertices, this yields a polynomial-time *exact* evaluation algorithm in the graph size n . Beyond Max-Cut, we extend the framework to general Binary Unconstrained Combinatorial Optimization (BUCO). Finally, we provide reproducible evaluations for rounds up to $p = 3$ on representative structured families, including the generalized Petersen graph $GP(15, 2)$, double-layer triangular 2-lifts, and the truncated icosahedron graph C_{60} , and report cut ratios while benchmarking against locality-matched classical baselines.

1 Introduction

The Quantum Approximate Optimization Algorithm (QAOA) [1], as a leading variational approach for combinatorial optimization, has attracted broad attention and has been applied to a range of problems, including Max-Cut and related constraint satisfaction tasks [1, 2, 3, 4]. Building on these applications, many efforts aim to improve QAOA’s empirical efficiency and solution quality via problem-tailored mixers and the Quantum Alternating Operator Ansatz [2], warm-start strategies [5, 6], annealing-based initialization [7], adaptive and counterdiabatic variants [8, 9], parameter-setting schemes for weighted instances [10], and hardware-scale studies that quantify execution-time and noise constraints for QAOA [11]. However, the assessment of these enhancements still relies predominantly on numerical benchmarks; beyond a few settings where guarantees can be inherited from classical relaxations or are proved for restricted graph families, rigorous, instance-wide performance bounds on general inputs remain scarce, so QAOA is still most often regarded as a heuristic quantum algorithm.

To obtain theoretical guarantees for QAOA, a basic objective is to understand the *expected* performance of *constant-round* QAOA, treating the number of alternating phase-mixer rounds p as a fixed constant. A central role is played by the QAOA expectation

$$\langle C \rangle = \langle \psi_p(\gamma, \beta) | C | \psi_p(\gamma, \beta) \rangle,$$

Shengminjie Chen: csmj@ict.ac.cn

which is both the objective optimized by classical parameter-tuning routines and the quantity whose value underpins approximation guarantees. In this work, we primarily focus on the Max-Cut objective, where C is the standard cut Hamiltonian on an input graph.

Farhi *et al.* [1] showed that one-round QAOA attains an approximation ratio of at least 0.6924 for Max-Cut on 3-regular graphs. Building on this, Wurtz and Love [12] proved worst-case approximation ratios of at least 0.7559 for $p = 2$ and 0.7924 for $p = 3$ on 3-regular graphs, the latter under a conjecture that graphs with no “visible” cycles are worst case. On sparse, locally tree-like inputs, constant-round QAOA has been analyzed from several angles : Basso *et al.* [13, 14] studied its performance on large sparse hypergraphs, mixed spin-glass models, and large-girth regular graphs, identifying both average-case limitations at fixed round and favorable high-round behavior on large-girth regular graphs and the Sherrington–Kirkpatrick model; Marwaha [15] and Hastings [16] showed that suitable local classical algorithms can match or even outperform low-round QAOA on high-girth regular graphs and on problems such as MAX-3-LIN-2 and triangle-free Max-Cut. More recently, Li *et al.* [17] moved beyond the high-girth regime by deriving an exact iterative formula for the expected cut fraction of (multi-angle) QAOA on certain low-girth expander graphs, and provided numerical evidence that constant-round QAOA and its variants can outperform the best-known classical local algorithms on these families.

Viewed through the lens of the expectation $\langle C \rangle$, many of these works share a common structure: they either derive explicit formulas or iterative schemes for $\langle C \rangle$ on particular graph families, or else bound it directly, and then translate these evaluations into approximation-ratio guarantees or comparisons with classical algorithms. From this perspective, understanding the performance of constant-round QAOA naturally leads to the classical problem of evaluating or approximating $\langle C \rangle$ as a function of the input instance and its structure.

Despite important progress in the theoretical performance analysis of QAOA, two fundamental questions remain open:

- **Structural solvability landscape.** On the algorithmic side, positive results for expectation evaluation are mostly known for graphs with additional structure, typically treated on a case-by-case basis using ad hoc combinatorial arguments or dynamic-programming techniques. These tractability results are scattered across particular graph families and are not organized by a unifying structural parameter such as treewidth, local treewidth (cf. [18, 19, 20]), or clique-/rank-width (cf. [21]), so they do not yet provide a parameter-driven picture that systematically explains when QAOA expectation evaluation should be feasible and when it should be intractable.
- **Expectation vs. sampling.** Within the QAOA literature, most rigorous complexity-theoretic results concern *sampling* tasks or individual output probabilities rather than expectation values. For example, even one-round QAOA can generate output distributions that are classically intractable to sample from under standard assumptions [22], and there are average-case hardness results for approximating output probabilities of random one-round QAOA circuits within additive error $2^{-O(n)}$ [23]. By contrast, despite the extensive work analyzing the approximation guarantees of constant-round QAOA on various graph and spin-glass ensembles (see the performance results discussed above), the classical complexity of evaluating the QAOA expectation at prescribed angles on general graphs for round $p \geq 2$ remains largely unresolved.

In this work, we try to answer the above two questions through a unified *complexity-algorithm* account of *constant-round* QAOA *expectation* computation. The main contributions are summarized as follows:

1. **Hardness on general graphs for round $p \geq 2$.** For Max-Cut on graphs and any round $p \geq 2$, exactly evaluating the QAOA expectation at prescribed angles is NP-hard, and even

achieving additive error at most $c2^{-2n}$ for some constant $c > 0$ is already NP-hard under this reduction. This directly targets the quantity optimized in practice and complements earlier results, which establish hardness of estimating output probabilities for single-round QAOA but do not address expectation values.

2. **Algorithmic-structural tractability and generalization.** We design an *iterative expectation evaluator* for constant p with total running time $\exp(O(p \cdot \text{ltw}_p(G))) \cdot \text{poly}(n)$, where $\text{ltw}_p(G)$ measures the treewidth of p -local graphs of G . On graph families whose local treewidth grows at most logarithmically in n , this yields *polynomial-time exact* expectations. The framework further *generalizes beyond Max-Cut* to BUCO via pseudo-Boolean expansions, yielding parallel evaluability guarantees in these settings.
3. **Reproducible experiments and locality-matched baselines.** We implement the p -local evaluator and report normalized expected cut ratios $\langle C \rangle / |E|$ for rounds up to $p = 3$ on three structured families (e.g., generalized Petersen graph $GP(15, 2)$, double-layer triangular 2-lifts, and truncated icosahedron graph C_{60}). To ensure fair comparison, we include classical k -local baselines matched to QAOA's lightcone radius (e.g., multi-step threshold-flip rules and Barak–Marwaha–type Gaussian-sum rules), enabling reproducible, like-for-like benchmarking of low round QAOA versus classical locality.

Organization. Sec. 2 fixes notation and structural parameters (including local treewidth). Sec. 3 proves NP-hardness of exact evaluation and shows that, for general graphs and any fixed round $p \geq 2$, approximating the expectation within additive error $2^{-O(n)}$ in the number of vertices n is already NP-hard. Sec. 4 presents the evaluator and its complexity guarantees and treats BUCO. Sec. 5 reports experiments on three structured families (Generalized Petersen graph $GP(15, 2)$, double-layer triangular 2-lifts, and truncated icosahedron graph C_{60}), followed by conclusions in Sec. 6.

2 PRELIMINARIES

This section introduces the basic notions of QAOA, together with auxiliary definitions needed in our proofs and algorithms. Throughout, we write $[n] = \{1, \dots, n\}$.

2.1 Definitions in Graph Theory

Let $G = (V, E)$ be a simple undirected graph with $n = |V|$ and $m = |E|$. For each node $v \in V$, let $N(v)$ denote the neighborhood set and $\deg(v) = |N(v)|$. For an edge $e = (u, v) \in E$ and integer $p \geq 0$, the p -hop vertex neighborhood represents the node set whose distance from u and v is not greater than p , i.e.,

$$N_p(e) = \{w \in V \mid \min(\text{dist}_G(u, w), \text{dist}_G(v, w)) \leq p\}. \quad (2.1)$$

where $\text{dist}_G(u, w)$ is distance between the node u and the node w . Normally, this distance is measured by the shortest path length in G from u to w . Leveraging the p -hop neighborhood set, the edge set of p -local subgraph $G_p(e)$ around the edge e is as follows:

$$E(G_p(e)) = \left\{ (x, y) \in E \mid \begin{array}{l} x, y \in N_p(e), \\ \min\{\text{dist}_G(u, x), \text{dist}_G(v, x), \text{dist}_G(u, y), \text{dist}_G(v, y)\} \leq p - 1 \end{array} \right\}. \quad (2.2)$$

For a vertex v , define $N_p(v)$ and $G_p(v)$ analogously.

As a natural extension of graphs, a hypergraph is $H = (V, \mathcal{E})$ with $\mathcal{E} \subseteq 2^V$. Its primal (Gaifman) graph $PG(H)$ connects $x, y \in V$ whenever there exists $f \in \mathcal{E}$ with $\{x, y\} \subseteq f$.

Neighborhoods and distances on H are taken via $PG(H)$. For a hyperedge $S \in \mathcal{E}$ and an integer $p \geq 0$, define the p -hop vertex neighborhood of S by

$$N_p^H(S) = \{v \in V : dist_{PG(H)}(v, S) \leq p\}, \quad dist_{PG(H)}(v, S) := \min_{u \in S} dist_{PG(H)}(u, v).$$

The corresponding p -local induced sub-hypergraph around S is

$$H_p(S) := H[N_p^H(S)],$$

that is, the sub-hypergraph of H with vertex set $N_p^H(S)$ and with hyperedge set $\{T \in \mathcal{E} : T \subseteq N_p^H(S)\}$.

2.2 QAOA and Its Expectation Performance

We briefly recall the QAOA ansatz for a combinatorial optimization problem. Consider an objective function $f(x)$ defined over n -bit strings, our goal is to find a bit string x such that $f(x)$ is as large as possible. Normally, the above function can be mapped into a Hamiltonian C that encodes function values for all possible input as a diagonal matrix in the computational basis, i.e.,

$$C|x\rangle = f(x)|x\rangle \quad \forall x \in \{0, 1\}^n$$

The QAOA ansatz at round $p \in \mathbb{N}$ is a general quantum algorithm for obtaining an approximate solution to a combinatorial optimization problem. Qubits are indexed by the bit set $[n]$. Starting from the uniform superposition over all computational basis states, i.e., $|+\rangle^{\otimes n} = \frac{1}{\sqrt{2^n}} \sum_{x \in \{0,1\}^n} |x\rangle$, QAOA alternates between using the phase operator with the parameter γ and the mixing operator with the parameter β , i.e.,

$$|\psi_p(\gamma, \beta)\rangle = U(B, \beta_p)U(C, \gamma_p) \cdots U(B, \beta_1)U(C, \gamma_1)|+\rangle^{\otimes n} = \left(\prod_{\ell=1}^p e^{-i\beta_\ell B} e^{-i\gamma_\ell C} \right) |+\rangle^{\otimes n}$$

where $U(B, \beta_p) = e^{-i\beta_p B} = \prod_{j \in [n]} e^{-i\beta_p X_j}$ is the mix operator, $U(C, \gamma_p) = e^{-i\gamma_p C}$ is the phase operator, and angles $(\gamma, \beta) \in \mathbb{R}^p \times \mathbb{R}^p$. Measuring the QAOA state $|\psi_p(\gamma, \beta)\rangle$ on the computational basis states, a good solution for combinatorial optimization problem can be recovered and its expected performance is as follows:

$$F_p(G; \gamma, \beta) = \langle \psi_p(\gamma, \beta) | C | \psi_p(\gamma, \beta) \rangle$$

Normally, obtaining the best angles is not easy. As an alternative, some suitable angles can be obtained by combining with the classical optimizer.

In special cases for Max-Cut, qubits are indexed by the node set V and the problem Hamiltonian (cost operator) aggregates edgewise parity penalties, while the mixer flips single qubit:

$$C = \sum_{(u,v) \in E} \frac{1 - Z_u Z_v}{2}, \quad B = \sum_{j \in V} X_j \quad (2.3)$$

It is convenient to decompose the cost into edge terms

$$C_e = \frac{1 - Z_u Z_v}{2}, \quad C = \sum_{e \in E} C_e, \quad (2.4)$$

Leveraging the above expression, the expected performance of QAOA for Max-Cut problem can be expressed as the sum of edgewise contributions, i.e.,

$$F_p(G; \gamma, \beta) = \sum_{e \in E} \langle \psi_p(\gamma, \beta) | C_e | \psi_p(\gamma, \beta) \rangle. \quad (2.5)$$

Evaluating each edge contribution through the Heisenberg-evolved observable $U_p^\dagger C_e U_p$ and exploiting the fact that this operator is supported only on the p -local graph $G_p(e)$ of e , we compute the edge contribution using only the restricted subcircuit on the subgraph $G_p(e)$:

$$\text{contrib}_p(e) = \langle + |^{\otimes |V(G_p(e))|} U_p^\dagger C_e U_p | + \rangle^{\otimes |V(G_p(e))|} \quad (2.6)$$

where $U_p = \prod_{\ell=1}^p e^{-i\beta_\ell B} e^{-i\gamma_\ell C}$, and $V(G_p(e))$ is the vertex set of $G_p(e)$. Summing $\text{contrib}_p(e)$ over $e \in E$ reproduces (2.5). The restricted subcircuit on the subgraph is normally referred as 'local-lightcone' evaluation that is the basis for our dynamic-programming algorithms and for the structural parameters introduced later.

In addition, the above formalism can be easily extended to weighted k -ary constraints. For a hypergraph $H = (V, \mathcal{E})$ with a hyperedge $f \subseteq V$ of arity $|f| \leq k$ and weight $w_f \geq 0$, define the parity penalty

$$C_f = \frac{w_f}{2} \left(1 - \prod_{i \in f} Z_i \right). \quad (2.7)$$

Taking $C = \sum_{f \in \mathcal{E}} C_f$ yields a QAOA instance for hypergraph Max-Cut-type objectives.

2.3 (Hyper)Tree Decompositions and Local Width

Tree decompositions capture how a graph can be assembled from small, overlapping pieces arranged along a tree; they provide the standard vehicle for dynamic programming on sparse structure. Let $H = (V_H, E_H)$ be a graph. A tree decomposition is a pair $(T, \{X_a\}_{a \in V(T)})$ whose nodes a are labelled by subsets ("bags") $X_a \subseteq V_H$ and that satisfies:

1. *Covering*: $\bigcup_a X_a = V_H$;
2. *Edge coverage*: for every $(x, y) \in E_H$ there exists $a \in V(T)$ with $\{x, y\} \subseteq X_a$;
3. *Running intersection*: for each $v \in V_H$, the set $\{a \in V(T) : v \in X_a\}$ induces a connected subtree of T .

The width of the decomposition is $\max_a |X_a| - 1$, and the treewidth $\text{tw}(H)$ is the minimum width over all decompositions [24]. Intuitively, small treewidth means that all interactions can be localized within small bags along a tree-shaped backbone.

For a hypergraph $H = (V, \mathcal{E})$ we adopt the standard convention that $\text{tw}(H) = \text{tw}(PG(H))$, where $PG(H)$ is the primal (Gaifman) graph on V with edges between any two vertices co-occurring in a hyperedge. Thus any tree decomposition of $PG(H)$ can be used verbatim for H : bags contain vertices, and every hyperedge is fully contained in some bags. This choice aligns the hypergraph case with our operator definitions based on Pauli Z -parities.

In light of the p -hop lightcone convention, we quantify the local structural complexity seen by an edge at depth p . For $p \geq 0$, define the p -local treewidth of G by

$$\text{ltw}_p(G) = \max_{e \in E} \text{tw}(G_p(e)). \quad (2.8)$$

For hypergraphs, ltw_p is computed on the primal graph $PG(H)$. By definition, $\text{ltw}_p(G)$ is monotone in p and bounded by the global treewidth ($\text{ltw}_p(G) \leq \text{tw}(G)$). This parameter measures the "hardest" p -local neighborhood and will govern the state size of our dynamic programs.

3 Inapproximability of the Expectation of Fixed-Round QAOA

In this section, we establish the computational complexity of evaluating the expected cut value of QAOA on Max-Cut, i.e., for any round $p \geq 2$, the exact evaluation problem given a graph G and angles (γ, β) is NP-hard. In addition, when assuming $\mathbf{P} \neq \mathbf{NP}$, no polynomial-time classical algorithm can approximate this expectation within additive error $2^{-O(n)}$. Our first formal statement is as follows:

Theorem 3.1 (Main Theorem). *For any round $p \geq 2$, if $\mathbf{P} \neq \mathbf{NP}$, then no classical polynomial-time algorithm can exactly compute the expected performance of QAOA for the Max-Cut problem at any arbitrarily given parameters (γ, β) .*

The key idea of the proof is to reduce an arbitrary graph G to a new graph G' . The construction ensures that, at QAOA round p , the local lightcone of the relevant observable spans the entire graph, so that the expectation of the cut objective encodes $\text{MAXCUT}(G')$; moreover, $\text{MAXCUT}(G)$ can be recovered from $\text{MAXCUT}(G')$ in polynomial time; then we rewrite (3.1) as a Laurent polynomial over the unit circle and show that its *largest nonzero exponent* encodes information about $\text{MAXCUT}(G')$. Leveraging the sampleability of $h(e^{i\phi})$, we can recover this exponent via a discrete inverse Fourier transform in polynomial time and thus obtain $\text{MAXCUT}(G)$. If the expected performance of QAOA for Max-Cut could be exactly computed in time polynomial in the graph size, this would contradict $P \neq NP$.

Proof. To begin the proof, we first present the definition of the expected value of QAOA. For a fixed constant $p \geq 2$, the QAOA expectation can be written as

$$\mathbb{E}[C] = \langle \gamma, \beta \mid C \mid \gamma, \beta \rangle. \quad (3.1)$$

In our proof, we choose a special parameter sequence with the assumption $\cos \psi \gg \sin \psi$ and $\cos \psi \geq 1 - 2^{-n^2}$ as below:

$$\beta = \left\{ \psi, \dots, \psi, \frac{\pi}{4}, \frac{\pi}{4} \right\}, \quad \gamma = \{\phi, \phi, \dots, \phi\},$$

where $n = |V(G')|$. Pick the exact dyadic angle $\psi := 2^{-\lceil n^2/2 \rceil} \in (0, \frac{\pi}{2})$. Using $\cos x \geq 1 - \frac{x^2}{2}$ we obtain

$$\cos \psi \geq 1 - \frac{\psi^2}{2} \geq 1 - 2^{-n^2}.$$

Here $\psi = 1/2^{\lceil n^2/2 \rceil}$ is dyadic, so its binary encoding length is $\Theta(n^2)$ bits. The constant π is fixed and independent of n , so no numerical-precision or encodability issues arise.

3.1 Graph Construction and Reduction ($G \rightarrow G'$)

First, we introduce the construction procedure for G' with $|V(G')| = n$ and $|E(G')| = m$. Let G be the original graph with $|V(G)| = n_0$ and $|E(G)| = m_0$ (assume G is connected). Construct G' as follows:

Vertex blow-up. For every vertex $u \in V$, create a bipartite complete graph $B(u) \cong K_{n_0+1, 10n_0}$, with bipartition (L_u, R_u) satisfying $|L_u| = n_0 + 1$ and $|R_u| = 10n_0$, and add all edges between L_u and R_u to E' . We fix an arbitrary but consistent labelling inside each gadget: we enumerate the left and right side as

$$L_u = \{u_{1,0}, u_{1,1}, \dots, u_{1,n_0}\}, \quad R_u = \{u_{2,0}, u_{2,1}, \dots, u_{2,10n_0-1}\}.$$

Here the first index (1 or 2) indicates whether the vertex lies in L_u or R_u , and the second index i records its position. All vertices of $B(u)$ are regarded as the replacement gadget for u .

Synchronous edges for original edges. For every original edge $(u, v) \in E$ and for every index $i \in \{0, 1, \dots, n_0\}$, add an edge $\{u_{1,i}, v_{1,i}\}$ between the i -th vertex of L_u and the i -th vertex of L_v . Thus each original edge generates $(n_0 + 1)$ parallel position-aligned edges. Insert all such edges into E' .

Global bipartite frame. Add an extra complete bipartite graph $K_{100n_0^2, 100n_0^2}$, whose two parts are

$$X = \{x_0, x_1, \dots, x_{100n_0^2-1}\}, \quad Y = \{y_0, y_1, \dots, y_{100n_0^2-1}\}.$$

Insert all edges of this bipartite graph into E' . Moreover, for every $u \in V$, connect the vertices $u_{1,i} \in L_u$ for $i \in [0, n_0]$ and $u_{2,j} \in R_u$ for $j \in [0, 10n_0 - 1]$ to both x_0 and y_0 .

Global controller. Add a new vertex w and connect it to x_0, y_0 , and every $u_{1,0}$ for $u \in V$. Insert all these edges into E' .

After the above four steps we obtain $V' = \bigcup_{u \in V} V(B(u)) \cup X \cup Y \cup \{w\}$, and the number of vertices is

$$|V'| = n_0((n_0 + 1) + 10n_0) + 200n_0^2 + 1 = 211n_0^2 + n_0 + 1.$$

We will present in Appendix A a polynomial-time procedure that recovers $\text{MAXCUT}(G)$ from $\text{MAXCUT}(G')$.

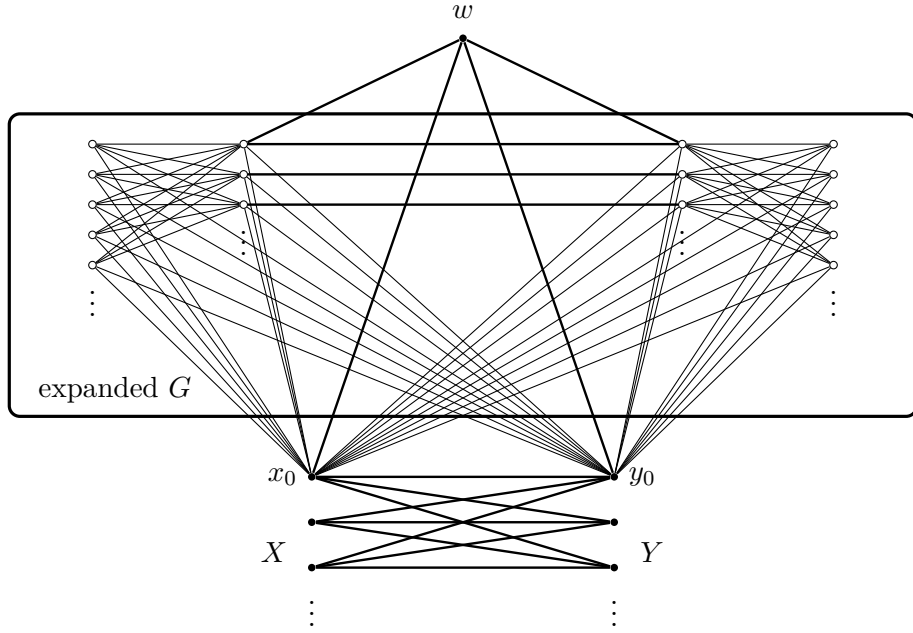


Figure 1: Construction of G' in the 2-vertex base case.

3.2 Laurent Polynomial Representation and Decomposition

Next, we introduce the expanding procedure for the expected performance of QAOA as a Laurent polynomial function. Firstly, we have

$$\langle \gamma, \beta | C | \gamma, \beta \rangle = \sum_{(u,v) \in E} \frac{1}{2} \langle \gamma, \beta | (1 - Z_u Z_v) | \gamma, \beta \rangle, \quad (3.2)$$

Using layer labels $j \in \{-p, \dots, -1, 0, 1, \dots, p\}$, a single term can be written as [14]:

$$\langle \gamma, \beta | Z_u Z_v | \gamma, \beta \rangle = \sum_{\{\mathbf{z}\}} z_u^{[0]} z_v^{[0]} \exp\left(i\phi \sum_{j=1}^p (C_j(\mathbf{z}) - C_{-j}(\mathbf{z}))\right) \prod_{v=1}^n f(\mathbf{z}_v), \quad (3.3)$$

where, for each vertex $u \in V$, we write

$$\mathbf{z}_u = (z_u^{[j]})_{j=-p}^p \in \{\pm 1\}^{2p+1}$$

for its spin values on the $2p + 1$ layers, and $\mathbf{z}^{[j]} = (z_u^{[j]})_{u \in V}$ denotes the spin configuration on layer j . The layer- j cut value is

$$C_j(\mathbf{z}) = \sum_{(p,q) \in E} \frac{1}{2} (1 - z_p^{[j]} z_q^{[j]}),$$

and the one-qubit mixer kernel is

$$f(\mathbf{z}_v) = \frac{1}{2} \langle z_v^{[1]} | e^{i\beta_1 X} | z_v^{[2]} \rangle \cdots \langle z_v^{[p]} | e^{i\beta_p X} | z_v^{[0]} \rangle \langle z_v^{[0]} | e^{-i\beta_p X} | z_v^{[-p]} \rangle \cdots \langle z_v^{[-2]} | e^{-i\beta_1 X} | z_v^{[-1]} \rangle.$$

The single-qubit matrix elements are

$$\langle u | e^{\pm i\beta_i X} | v \rangle = \begin{cases} \cos \beta_i, & u = v, \\ \pm i \sin \beta_i, & u \neq v. \end{cases}$$

Detailed derivations of (3.3) can be found in Appendix B. Formally, the above equation can be reformulated into the Laurent polynomial function as below:

$$\langle Z_u Z_v \rangle = \langle \gamma, \beta | Z_u Z_v | \gamma, \beta \rangle = h_{(u,v)}(e^{i\phi}), \quad (3.4)$$

$$h_{(u,v)}(x) = \sum_{k=-m}^m w(k) x^k, \quad (3.5)$$

with m the maximal possible degree and $w(k)$ the coefficients. Hence

$$\langle \gamma, \beta | C | \gamma, \beta \rangle = -\frac{1}{2} h(e^{i\phi}) + c_0 = -\frac{1}{2} \sum_{(u,v) \in E} h_{(u,v)}(e^{i\phi}) + c_0. \quad (3.6)$$

where $c_0 = \sum_{(u,v) \in E} \frac{1}{2} = \frac{m}{2}$ is a constant.

3.3 The Polynomial $h_{(x_0, y_0)}$ Induced by the Observable $Z_{x_0} Z_{y_0}$

Since the Laurent polynomial for the global observable $C(\mathbf{z})$ decomposes into a sum of Laurent polynomials associated with single-edge observables, we therefore first focus on the edge polynomial $h_{(x_0, y_0)}(x)$ induced by $Z_{x_0} Z_{y_0}$, with particular attention to its *largest nonzero exponent*. For convenience, we denote a possible assignment for $\mathbf{z} = \{z_i\}$ where $z_i \in \{\pm 1\}^{2p+1} \forall i \in V$ as a configuration. The detailed proof of lemmas in this subsection can be referred in Appendix C.

Before describing the largest nonzero exponent, we first introduce the Endpoint consistency phenomenon for each observable $Z_u Z_v$, which can make us ignore many items.

Lemma 3.2 (Endpoint consistency). *For any vertex q , the dependence of the contribution to $\langle Z_u Z_v \rangle$ on $z_q^{[0]}$ falls into the following cases:*

1. *If $q \notin \{u, v\}$ and $z_q^{[p]} \neq z_q^{[-p]}$, then replacing $z_q^{[0]}$ by $-z_q^{[0]}$ flips the sign of the contribution. The two configurations related by this flip therefore cancel in the sum.*
2. *If $q \in \{u, v\}$ and $z_q^{[p]} = z_q^{[-p]}$, then flipping $z_q^{[0]}$ again flips the sign of the contribution, so the corresponding pair of configurations cancels.*
3. *In all remaining cases (that is, when $q \notin \{u, v\}$ with $z_q^{[p]} = z_q^{[-p]}$, or $q \in \{u, v\}$ with $z_q^{[p]} \neq z_q^{[-p]}$), the contribution is independent of $z_q^{[0]}$.*

Intuitively, once endpoint-consistency is imposed and since all cost layers are diagonal in the Z basis, the only dependence on the layer-0 spin of a given vertex q comes from the two end-layer mixers on q (and, when $q \in \{u, v\}$, from the observable factor $z_u^{[0]} z_v^{[0]}$). At the boundary $\beta_p = \frac{\pi}{4}$ the relevant one-qubit matrix elements of $e^{\pm i\beta_p X}$ all have the same magnitude and differ only by a sign, so flipping $z_q^{[0]}$ either flips an overall sign (cases (1)–(2), giving pairwise cancellation) or leaves the contribution unchanged (case (3)), exactly as stated in the lemma.

Lemma 3.3 (No high-degree contribution under asynchronous flips). *For the observable $Z_{x_0} Z_{y_0}$, if $z_{x_0}^{[p]} \neq z_{y_0}^{[p]}$, then there is no contribution to coefficients with exponents*

$$k \geq \left((p-1) \text{MC} + 200n_0^2 + 2n_0(11n_0 + 1) \right),$$

where $\text{MC} := \text{MAXCUT}(G')$. Using the symmetry and cancellation above, configurations that can attain the *largest nonzero exponent* and are non-negligible can be restricted to: taking a same maximum-cut assignment on layers $[1, p-1]$, a same minimum-cut assignment on layers $[-p+1, -1]$, and then using the boundary layers $(p, 0, -p)$ to achieve the largest exponent. Concretely, let $C_j(\mathbf{z})$ and $C_{-j}(\mathbf{z})$ be a common maximum cut and a minimum cut for $j \in \{1, 2, \dots, p-1\}$, respectively. Adjusting the spins at layers $p, 0, -p$ yields a nonzero largest term. At layer p we set x_0, y_0 to be opposite to w and the rest to agree with w , while at layer $-p$ we flip both x_0, y_0 and keep all the other vertices identical to those at layer p . Under this operation, the largest exponent becomes $\left((p-1) \text{MC} + 200n_0^2 + 2n_0(11n_0 + 1) \right)$. In addition, we also have an observation that edges other than (x_0, y_0) will not contribute to the largest nonzero exponent. The formal statement is as follows:

Lemma 3.4 (largest nonzero exponent). *For the observable $Z_{x_0} Z_{y_0}$, the largest nonzero exponent in $h_{(x_0, y_0)}$ attainable by the induced polynomial is*

$$\left((p-1) \text{MC} + 200n_0^2 + 2n_0(11n_0 + 1) \right). \quad (3.7)$$

Lemma 3.5 (Lower bound for other edges). *Let the observable be $Z_i Z_j$ with $(i, j) \notin \{(x_0, y_0), (y_0, x_0)\}$. Then all coefficients of the terms in $h_{(i, j)}$ with exponents $\geq \left((p-1) \text{MC} + 200n_0^2 + 2n_0(11n_0 + 1) \right)$ vanish.*

Combining the above lemmas, the main remaining obstacle has become the calculation for the largest nonzero exponent of h . It reduces to consider the largest nonzero exponent of $h_{(x_0, y_0)}$, i.e., $\left((p-1) \text{MC} + 200n_0^2 + 2n_0(11n_0 + 1) \right)$.

3.4 Sampling on the Unit Circle and FFT Interpolation: Recovering Max-Cut from the Exponent

Leveraging the aforementioned statements, we illustrate that the largest nonzero exponent of h is $D_{\max} = \left((p-1) \text{MC} + 200n_0^2 + 2n_0(11n_0 + 1) \right)$. Next, we introduce the recovering procedure for MC from the exponent.

On the $(2m+1)$ -st roots of unity $\omega = e^{2\pi i/(2m+1)}$, choose the $2m+1$ equally spaced points $x_j = \omega^j$ for $j = -m, \dots, m$. Then

$$-\frac{1}{2}h(x_j) + c_0 = -\frac{1}{2} \sum_{k=-m}^m w(k) \omega^{jk} + c_0 = \sum_{k=-m}^m w_1(k) \omega^{jk}. \quad (3.8)$$

where c_0 is a known constant. Let $\mathcal{F}(x) = x^m(-\frac{1}{2}h(x) + c_0)$. Given the sequence $\mathcal{F}(x_j)$, the inverse FFT yields

$$w_1(k-m) = \frac{1}{2m+1} \sum_{j=0}^{2m} \mathcal{F}(x_j) \omega^{-jk}, \quad k = 0, 1, \dots, 2m, \quad (3.9)$$

so that all coefficients $\{w_1(k)\}$ are recovered in time $O(m \log m)$. By Lemmas 3.4 and 3.5, the *largest nonzero exponent* is uniquely determined by the $Z_{x_0} Z_{y_0}$ -induced term; therefore, we can obtain D_{\max} by finding the term with the highest degree that has a non-zero coefficient, obtain $\text{MC} = \text{MAXCUT}(G')$, and then recover $\text{MAXCUT}(G)$. If a classical polynomial-time algorithm could compute (3.1) for arbitrary (γ, β) , then the above would yield a polynomial-time algorithm for Max-Cut on arbitrary graphs, contradicting $\mathbf{P} \neq \mathbf{NP}$. This proves Theorem 3.1. \square

3.5 Inapproximability under Additive Error

We now derive hardness-of-approximation consequences from the coefficient-recovery argument based on the inverse transform (3.9).

We will use the following standing lemma.

Lemma 3.6 (Gap at the top degree). *There exists a constant $c > 0$ (independent of n when n is large enough) such that the coefficient at the largest nonzero exponent D_{\max} satisfies $|w(D_{\max})| = |-2w_1(D_{\max})| \geq c \cdot 2^{-2n}$.*

The detailed proof of this lemma is deferred to Appendix C. We now begin the proof of the Corollary 3.7.

Corollary 3.7 (Additive-error bound). *For any fixed round $p \geq 2$, if $\mathbf{P} \neq \mathbf{NP}$ then there exists a constant $c' > 0$ (independent of n) such that no classical polynomial-time algorithm can, for arbitrarily prescribed parameters (γ, β) , approximate (3.1) on n -vertex instances within additive error $c'2^{-2n}$.*

Proof. Write $h(x)$ for the Laurent polynomial in (3.1) so that $\langle C \rangle = -\frac{1}{2}h(e^{i\phi}) + c_0$. As established in Sec. 3, the support of h lies in $\{-m, \dots, m\}$. Let $\mathcal{F}(x) := x^m(-\frac{1}{2}h(x) + c_0) = \sum_{k=0}^{2m} w_1(k-m) x^k$ be the associated ordinary polynomial, and let $\omega := e^{2\pi i/(2m+1)}$.

Consider any putative polynomial-time approximator \mathcal{A} for (3.1) at (γ, β) . On input the $2m+1$ angles $\phi_j := \frac{2\pi j}{2m+1}$, it returns values $\langle C \rangle^*(\omega^j)$ obeying

$$|\langle C \rangle^*(\omega^j) - \langle C \rangle(\omega^j)| \leq \varepsilon \quad \text{for all } j \in \{0, \dots, 2m\}.$$

Since $|\omega^j| = 1$, setting $\mathcal{F}^*(\omega^j) := (\omega^j)^m (\langle C \rangle^*(\omega^j))$ gives

$$\mathcal{F}^*(\omega^j) = \mathcal{F}(\omega^j) + \eta_j, \quad |\eta_j| \leq \varepsilon.$$

Recover the coefficients by the inverse DFT (3.9):

$$w_1^*(k-m) = \frac{1}{2m+1} \sum_{j=0}^{2m} \mathcal{F}^*(\omega^j) \omega^{-jk}.$$

Averaging preserves the uniform error, hence for every k ,

$$|w_1^*(k-m) - w_1(k-m)| \leq \frac{1}{2m+1} \sum_{j=0}^{2m} |\eta_j| \leq \varepsilon. \quad (3.10)$$

Choose $\varepsilon \leq (c/3) 2^{-2n}$. Since D_{\max} is the *largest* index with a nonzero coefficient, all degrees $> D_{\max}$ have coefficient 0, while $|w_1(D_{\max})| \geq c 2^{-2n}$ by Lemma 3.6 (c is a constant). By (3.10) we then have

$$\begin{cases} |w_1^*(s)| \leq \varepsilon \leq (c/3) 2^{-2n}, & \text{for all } s > D_{\max}, \\ |w_1^*(D_{\max})| \geq |w_1(D_{\max})| - \varepsilon \geq (2c/3) 2^{-2n}. \end{cases}$$

Therefore, scanning indices from m downward and thresholding at $\tau := (c/2) 2^{-2n}$, the first index whose estimated magnitude exceeds τ is *exactly* D_{\max} .

Finally, by Lemma 3.4, D_{\max} is an explicit affine function of the MAXCUT value (with fixed coefficients depending only on p and the normalization), so this procedure recovers MAXCUT in classical polynomial time, contradicting $\mathbf{P} \neq \mathbf{NP}$. \square

This corollary can be naturally extended to its quantum version. Assuming $\mathbf{NP} \not\subseteq \mathbf{BQP}$, for any fixed $p \geq 2$ there is also no BQP algorithm that, for arbitrarily prescribed $(\boldsymbol{\gamma}, \boldsymbol{\beta})$, approximates (3.1) within additive error $c' 2^{-2n}$. Since we did not require the machines to be quantum or classical in our previous arguments, therefore achieving accuracy $\leq c' 2^{-2n}$ would let us solve Max-Cut which would conflict with $\mathbf{NP} \not\subseteq \mathbf{BQP}$.

4 QAOA Expectation with Tree Decomposition

In this section, we first present a *bag-level dynamic programming (DP)* framework leveraging tree decomposition to exactly calculate the expectation of QAOA, which also suffers from the hardness result in the above section. We also extend our algorithm to evaluate the expectation of QAOA for general combinatorial optimization problems.

4.1 Bag-Level Dynamic Programming

Recalling the definition of the expectation for QAOA with the constant round p on a general graph, it can be reformulated as a sum of strictly p -local contributions for each edge. Considering the edge $e = (l, r)$ with weight w_{lr} and its radius- p induced subgraph $G_p(e)$, the contribution for the edge e is as below:

$$\text{contrib}_p(e) = \sum_{\{\mathbf{z}_v : v \in V(G_p(e))\}} \left[\frac{w_{lr}}{2} (1 - z_l^{[0]} z_r^{[0]}) \right] \exp\left(i \sum_{j=-p}^p \Gamma_j C_{G_p(e)}(z^{[j]})\right) \prod_{v \in V(G_p(e))} f(\mathbf{z}_v) \quad (4.1)$$

where $\boldsymbol{\Gamma} = \{\gamma_1, \dots, \gamma_p, 0, -\gamma_p, \dots, -\gamma_1\}$ collects the angle coefficients, $C_{G_p(e)}(\cdot)$ is the cut on $G_p(e)$, and $f(\cdot)$ is the one-site mixer kernel.

High-level idea. Fix a round p and angles $(\boldsymbol{\gamma}, \boldsymbol{\beta})$. For each edge $e = (l, r)$ let $G_p(e)$ be the graph induced radius- p neighborhood of (l, r) . By finite lightcones, the Heisenberg-evolved edge observable $F_p(G; \boldsymbol{\gamma}, \boldsymbol{\beta})$ has support contained in $G_p(e)$, so the objective splits into strictly p -local edge contributions. A *volume-based* baseline evaluates each $F_p(G; \boldsymbol{\gamma}, \boldsymbol{\beta})$ by enumerating all spins on $V(G_p(e))$, paying $2^{|V(G_p(e))|}$. Our approach is *separator-based* by equipping $G_p(e)$ with a tree decomposition and viewing bag intersections as *separators*. Conditioning on a separator fixes the interface to descendants so that interior spins factor; we cache the resulting partial sums as *messages* indexed by separator assignments by using dynamic programming on the decomposition. This replaces the exponential dependence on the *volume* $|V(G_p(e))|$ by an exponential in the *local treewidth* $\text{tw}(G_p(e))$: the per-edge cost is polynomial in $|G|$ and singly exponential in $(p, \text{tw}(G_p(e)))$ (e.g., $2^{O((\text{tw}(G_p(e))+1) \cdot p)}$ up to polynomial factors), rather than $2^{|V(G_p(e))|}$. Hence, whenever $G_p(e)$ admits small separators, DP reuses sub-computations across the exponentially many global assignments and yields exponential savings over brute force; when $\text{tw}(G_p(e))$ is

Algorithm 1 ComputeQAOAExpectation(G, γ, β, p)

Input: a graph $G = (V, E)$, angles γ, β , and round p
Output: unnormalized expectation Ex of QAOA on G

```

1:  $Ex \leftarrow 0$ 
2: for all  $e = (u, v) \in E$  do
3:    $H \leftarrow \text{BFSSUBGRAPH}(G, e, p)$             $\triangleright p\text{-local subgraph } G_p(e) \text{ as defined in (2.1)–(2.2)}$ 
4:    $(T, \{X_a\}_{a \in V(T)}) \leftarrow \text{KORHONEN2APPROXTD}(H)$ 
5:    $\Delta \leftarrow \text{DPONDECOMPOSITION}(H, T, \{X_a\}, \gamma, \beta, e)$ 
6:    $Ex \leftarrow Ex + \Delta$ 
7: end for
8: return  $Ex$ 

```

large the algorithm degrades gracefully toward the natural exponential baseline while remaining exact. The pseudocode of the bag-level dynamic program is given in Algorithm 1.

The subsequent subsection details the bag messages, separator structure, and the root assembly used by DPONDECOMPOSITION, which implements (4.1) exactly on the chosen tree decomposition.

4.2 DP on a Tree Decomposition and Root Assembly

For convenience, we say that edge (x, y) belongs to bag X if and only if X contains both vertices x and y . When considering the contribution of the edge (l, r) , the root of tree decomposition is a bag *root* that contains the edge (l, r) . For a directed edge $(a \rightarrow \text{pa}(a))$ in the tree decomposition $(T, \{X_a\}_{a \in V(T)})$, we define the separator $S_a = X_a \cap X_{\text{pa}(a)}$ (with $S_{\text{root}} = \emptyset$) and introduce the notation of vertices and *top edges* of each bag:

$$V_a = \{u \in X_a : \text{top}(u) = a\}, \quad E_a = \{(u, v) \in X_a : \text{top}((u, v)) = a\},$$

where $\text{top}(\cdot)$ is the bag closest to the root within the connected subtree of bags containing the item.

Given a separator assignment $\mathbf{z}_{S_a} = \{z_u^{[j]} \in \{\pm 1\} : u \in S_a, j = -p, \dots, p\}$, define the *bag message* (bottom-up):

$$g(a, \mathbf{z}_{S_a}) = \sum_{\mathbf{z}_{V_a}} \left[\underbrace{\left(\prod_{u \in V_a} f(z_u) \right)}_{\text{vertex kernels settled at } V_a} \cdot \underbrace{\exp\left(i \sum_{j=-p}^p \Gamma_j C_{E_a}(\mathbf{z}^{[j]})\right)}_{\text{edge phases settled at } E_a} \cdot \prod_{b \in \text{child}(a)} g(b, \mathbf{z}_{S_b}) \right] \quad (4.2)$$

where $C_{E_a}(\mathbf{z}^{[j]}) = \sum_{(x,y) \in E_a} \frac{w_{xy}}{2} (1 - z_x^{[j]} z_y^{[j]})$. If a is leaf-bag, we set $\prod_{b \in \text{child}(a)} g(b, \mathbf{z}_{S_b}) = 1$. For the *root* bag, we can obtain the contribution of the edge (l, r) from the message at its child.

$$\begin{aligned} \text{contrib}_p(e) &= \sum_{\mathbf{z}_{X_{\text{root}}}} \underbrace{\frac{w_{lr}}{2} (1 - z_l^{[0]} z_r^{[0]})}_{\text{measurement factor}} \left(\prod_{u \in V_{\text{root}}} f(z_u) \right) \\ &\quad \times \exp\left(i \sum_{j=-p}^p \Gamma_j C_{E_{\text{root}}}(\mathbf{z}^{[j]})\right) \prod_{b \in \text{child}(\text{root})} g(b, \mathbf{z}_{S_b}) \end{aligned} \quad (4.3)$$

Correctness. By the running-intersection property of the tree decomposition, for every vertex u (resp. edge (l, r)), bags containing it form a connected subtree of T . Writing $\text{top}(u)$ and $\text{top}((l, r))$ for the unique bags in those subtrees closest to the root. The families $\{V_a\}_{a \in V(T)}$ and $\{E_a\}_{a \in V(T)}$ are pairwise disjoint and satisfy $\cup_a V_a = V(G_p(e))$ and $\cup_a E_a = E(G_p(e))$, respectively.

Fix any bag a and separator assignment \mathbf{z}_{S_a} . The message $g(a, \mathbf{z}_{S_a})$ defined by the bag–message recurrence (4.2) equals the sum, over all copy variables in $\text{subtree}(a)$ that extend \mathbf{z}_{S_a} , of the integrand obtained by multiplying: (i) for each vertex u in the subtree, the one–site kernel $f(\mathbf{z}_u)$ exactly once, counted at $\text{top}(u)$; and (ii) for each edge (l, r) in the subtree, the phase $\exp(i \sum_j \Gamma_j C_{(l,r)}(\mathbf{z}^{[j]}))$ exactly once, counted at $\text{top}((l, r))$. This is proved by a bottom–up induction on T : the leaf case is immediate from (4.2); for the inductive step, child subtrees are glued along separators $X_b \cap X_a$, and the running–intersection property guarantees cross–bag consistency so that each vertex kernel and edge phase is accounted for exactly once. At the root, the assembly step (4.3) inserts the observable for the chosen edge e and sums over $\mathbf{z}_{X_{\text{root}}}$, thereby reproducing the localized objective exactly.

Algorithm 2 DPOnDecomposition($H, T, \{X_a\}, \gamma, \beta, e = (l, r)$)

Input: induced subgraph H , tree decomposition $(T, \{X_a\})$, angles (γ, β) , edge $e = (l, r)$
Output: $\text{contrib}_p(e)$

- 1: **postorder-traverse** T from leaves to the root root (with $\{l, r\} \subseteq X_{\text{root}}$)
- 2: **for all** bags a in postorder **do**
- 3: compute the message $g(a, \mathbf{z}_{S_a})$ via the bag recurrence
- 4:
$$g(a, \mathbf{z}_{S_a}) = \sum_{\mathbf{z}_{V_a}} \left[\prod_{u \in V_a} f(z_u) \right] \exp \left(i \sum_{j=-p}^p \Gamma_j C_{E_a}(\mathbf{z}^{[j]}) \right) \prod_{b \in \text{child}(a)} g(b, \mathbf{z}_{S_b})$$
- 5: **end for**
- 6: assemble at the root root obtaining $\text{contrib}_p(e)$ by (4.3)
- 7: **return** $\text{contrib}_p(e)$

Next, we discuss the complexity of the algorithm. For convenience, denote $L := 2p + 1$.

Per-subgraph parameters. For a p -local subgraph $G_p(e)$, let $\tilde{\text{tw}}(G_p(e))$ be the width of the tree decomposition actually used by the DP. Using the 2-approximation for treewidth [25], we obtain $\tilde{\text{tw}}(G_p(e)) \leq 2 \text{tw}(G_p(e)) + 1$.

Building neighborhoods and TDs. Extracting the radius- p neighborhood $G_p(e)$ by BFS takes $\tilde{O}(|V(G_p(e))| + |E(G_p(e))|)$ time. Computing a 2-approximate tree decomposition (TD) for $G_p(e)$ takes $\tilde{O}(|V(G_p(e))| \cdot 2^{O(\text{tw}(G_p(e)))})$ time and returns width $\leq 2\text{tw}(G_p(e)) + 1$.

Per-subgraph DP. Process the TD in postorder. A bag with at most $\tilde{\text{tw}}(G_p(e)) + 1$ vertices has $2^{L(\tilde{\text{tw}}(G_p(e)) + 1)}$ assignments of replicated spins. Since each local kernel/phase and child message is aggregated only once, from an amortized perspective, each table entry aggregates $O(1)$ local kernels/phases and $O(1)$ child messages, and this process must be carried out after pretabulation, hence

$$\begin{aligned} T_{\text{DP}}(G_p(e)) &= 2^{L(\tilde{\text{tw}}(G_p(e)) + 1)} \cdot \tilde{O}(|V(G_p(e))| + |E(G_p(e))|) \\ S_{\text{DP}}(G_p(e)) &= 2^{L(\tilde{\text{tw}}(G_p(e)) + 1)} \cdot \tilde{O}(|V(G_p(e))|) \end{aligned}$$

Total over all edges. For $G_p(e)$, write $n_e := |V(G_p(e))|$, $m_e := |E(G_p(e))|$, $t_e := \text{tw}(G_p(e))$, $w_e := \tilde{\text{tw}}(G_p(e))$, and define

$$N := \sum_e n_e, \quad M := \sum_e m_e, \quad t := \max_e t_e, \quad w := \max_e w_e.$$

Summing the three components (neighborhood extraction, TD, DP) gives

$$T_{\text{total}} \leq \underbrace{\tilde{O}(N + M)}_{\text{build all } G_p(e)} + \underbrace{\tilde{O}(N \cdot 2^{O(t)})}_{\text{TD 2-approx}} + \underbrace{2^{L(w+1)} \cdot \tilde{O}(N + M)}_{\text{all bag-DP work}} \quad (4.4)$$

In particular, for fixed p the DP term dominates asymptotically, and

$$T_{\text{total}} = 2^{L(w+1)} \cdot \tilde{O}(N + M) + (\text{lower-order terms}).$$

The peak working space is $S_{\text{total}} = 2^{L(w+1)} \cdot \tilde{O}(N)$.

Bounded local treewidth (fixed p). If the instance family has bounded local treewidth, i.e., $t = \max_e t_e = O(1)$, then also $w = O(1)$ for the 2-approx TD (and $w = t$ for exact TDs). Hence $T_{\text{total}} = \text{poly}(N)$, $S_{\text{total}} = \text{poly}(N)$.

4.3 Generalization to Binary Unconstrained Combinatorial Optimization

We now show that the p -local DP framework developed for graph Max-Cut extends, with minimal changes, to general binary unconstrained combinatorial optimization (BUCO). We first express a BUCO instance in a standard pseudo-Boolean form and encode it as a hypergraph cut; in this way, the relevant locality and width parameters are inherited by the primal graph of the induced p -local subinstances. Throughout this subsection we reuse the notation for replicated layers, angle coefficients Γ , and the single-qubit mixer kernel $f(\cdot)$ from Secs. 2 and 4.

Any BUCO objective admits the pseudo-Boolean expansion

$$C_B(\mathbf{z}) = c_0 + \sum_j c_j z_j + \sum_{j < k} c_{jk} z_j z_k + \sum_{j < k < \ell} c_{jkl} z_j z_k z_\ell + \dots, \quad z_i \in \{\pm 1\}, \quad (4.5)$$

where the sum ranges over all nonempty subsets $S \subseteq V$ and $c_S \in \mathbb{R}$ are (real) coefficients. The corresponding target Hamiltonian is

$$C_B = c_0 I + \sum_{S \neq \emptyset} c_S \prod_{i \in S} Z_i. \quad (4.6)$$

Grouping monomials by their support, let

$$\mathcal{E} := \{S \subseteq V : c_S \neq 0\}$$

and define a hypergraph $H = (V, \mathcal{E})$ whose hyperedges are the supports S of nonzero monomials. For each $S \in \mathcal{E}$ set

$$w_S := -2c_S$$

and view $w_S \in \mathbb{R}$ as a weight on S . The associated hypergraph cut objective and Hamiltonian are defined by

$$C_H(\mathbf{z}) = \frac{1}{2} \sum_{S \in \mathcal{E}} w_S \left(1 - \prod_{u \in S} z_u\right), \quad z_u \in \{\pm 1\}, \quad (4.7)$$

$$C_H = \frac{1}{2} \sum_{S \in \mathcal{E}} w_S \left(1 - \prod_{u \in S} Z_u\right). \quad (4.8)$$

A direct calculation shows that for every spin configuration \mathbf{z} ,

$$C_H(\mathbf{z}) = \frac{1}{2} \sum_{S \in \mathcal{E}} w_S - \frac{1}{2} \sum_{S \in \mathcal{E}} w_S \prod_{u \in S} z_u = - \sum_{S \in \mathcal{E}} c_S + \sum_{S \in \mathcal{E}} c_S \prod_{u \in S} z_u.$$

Thus

$$C_B(\mathbf{z}) = c_0 + \sum_{S \in \mathcal{E}} c_S \prod_{u \in S} z_u = c_* + C_H(\mathbf{z}), \quad c_* := c_0 + \sum_{S \in \mathcal{E}} c_S.$$

In particular, C_B and C_H differ only by an additive constant, so they have the same maximizers:

$$\arg \max_{\mathbf{z}} C_B(\mathbf{z}) = \arg \max_{\mathbf{z}} C_H(\mathbf{z}), \quad \max_{\mathbf{z}} C_B(\mathbf{z}) = c_* + \max_{\mathbf{z}} C_H(\mathbf{z}).$$

At the Hamiltonian level we likewise have

$$C_B = c_* I + C_H,$$

so for any QAOA state $|\psi_p\rangle$ the expectations are related by

$$\langle \psi_p | C_B | \psi_p \rangle = c_* + \langle \psi_p | C_H | \psi_p \rangle.$$

That is, evaluating the BUCO objective under QAOA is equivalent (up to an additive constant) to evaluating the weighted hypergraph cut objective C_H , namely the total weight of cut hyperedges.

Hence, in the remainder of this subsection we focus on the hypergraph cut form (4.8). Fix a hyperedge $S_0 \in \mathcal{E}$ and write the corresponding observable as

$$\mathcal{O}_{S_0} = \frac{w_{S_0}}{2} \left(1 - \prod_{i \in S_0} Z_i \right).$$

We let $H_{S_0} = H_p(S_0)$ denote the induced p -local sub-hypergraph defined in Sec. 2. With the layer spins $\mathbf{z}^{[j]}$ and the single-site kernel $f(\cdot)$ as in Appendix B, the localized formula is

$$\langle \psi_p | \mathcal{O}_{S_0} | \psi_p \rangle = \sum_{\{\mathbf{z}_v : v \in V(H_{S_0})\}} \frac{w_{S_0}}{2} \left(1 - \prod_{i \in S_0} z_i^{[0]} \right) \exp \left(i \sum_{j=-p}^p \Gamma_j C_{H_{S_0}}(\mathbf{z}^{[j]}) \right) \prod_{v \in V(H_{S_0})} f(\mathbf{z}_v), \quad (4.9)$$

where

$$C_{H_{S_0}}(\mathbf{z}^{[j]}) = \frac{1}{2} \sum_{S \in \mathcal{E}(H_{S_0})} w_S \left(1 - \prod_{u \in S} z_u^{[j]} \right).$$

On the hypergraph H_{S_0} , take a graph tree decomposition $(T, \{X_a\})$ of the primal graph $PG(H_{S_0})$ such that every hyperedge $S \in \mathcal{E}(H_{S_0})$ is contained in at least one bag X_a (here we say a hyperedge S belongs to X_a if and only if X_a contains all vertices in S) and the running-intersection property holds. Choose a root bag $root$ with $S_0 \subseteq X_{root}$. For each arc $(a \rightarrow pa(a))$, set $S_a = X_a \cap X_{pa(a)}$ and $V_a = X_a \setminus S_a$. Define the set of hyperedges introduced at a by

$$\mathcal{E}_a = \{ S \in \mathcal{E}(H_{S_0}) : S \subseteq X_a, S \not\subseteq X_{pa(a)} \}. \quad (4.10)$$

For a separator configuration \mathbf{z}_{S_a} , define the bag message

$$g(a, \mathbf{z}_{S_a}) = \sum_{\mathbf{z}_{V_a}} \left[\prod_{u \in V_a} f(\mathbf{z}_u) \exp \left(i \sum_{j=-p}^p \Gamma_j C_{\mathcal{E}_a}(\mathbf{z}^{[j]}) \right) \prod_{b \in \text{child}(a)} g(b, \mathbf{z}_{S_b}) \right], \quad (4.11)$$

where

$$C_{\mathcal{E}_a}(\mathbf{z}^{[j]}) = \frac{1}{2} \sum_{S \in \mathcal{E}_a} w_S \left(1 - \prod_{u \in S} z_u^{[j]} \right). \quad (4.12)$$

If a is a leaf bag, we set

$$\prod_{b \in \text{child}(a)} g(b, \mathbf{z}_{S_b}) = 1.$$

The root assembly is

$$\begin{aligned} \langle \psi_p | \mathcal{O}_{S_0} | \psi_p \rangle &= \sum_{\mathbf{z}_{X_{root}}} \frac{w_{S_0}}{2} \left(1 - \prod_{i \in S_0} z_i^{[0]} \right) \left[\prod_{u \in V_{root}} f(\mathbf{z}_u) \right] \\ &\quad \times \exp \left(i \sum_{j=-p}^p \Gamma_j C_{\mathcal{E}_{root}}(\mathbf{z}^{[j]}) \right) \prod_{b \in \text{child}(root)} g(b, \mathbf{z}_{S_b}). \end{aligned} \quad (4.13)$$

We next analyse the time complexity of the hypergraph algorithm.

Algorithm 3 ComputeQAOAExpectation–BUCO (C_B, γ, β, p)

Input: BUCO objective $C_B(z) = c_0 + \sum_{S \neq \emptyset} c_S \prod_{i \in S} z_i$ on spins $z_i \in \{\pm 1\}$, angles (γ, β) , round p

Output: $F_p(C_B; \gamma, \beta) = \langle \psi_p | C_B | \psi_p \rangle$

- 1: Construct the hypergraph $H = (V, \mathcal{E})$ with one hyperedge $S \in \mathcal{E}$ for each nonzero monomial $c_S \prod_{i \in S} z_i$, and set $w_S \leftarrow -2c_S$
- 2: $c_* \leftarrow c_0 + \sum_{S \in \mathcal{E}} c_S$
- 3: $Ex \leftarrow c_*$ // constant shift: $C_B = c_* I + C_H$
- 4: **for all** $S_0 \in \mathcal{E}$ **do**
- 5: $H_{S_0} \leftarrow H_p(S_0)$
- 6: Compute a tree decomposition $(T, \{X_a\})$ of $PG(H_{S_0})$ with a root bag $root$ such that $S_0 \subseteq X_{root}$
- 7: $\Delta \leftarrow \langle \psi_p | \mathcal{O}_{S_0} | \psi_p \rangle$ via bag messages and root assembly (4.11)–(4.13)
- 8: $Ex \leftarrow Ex + \Delta$
- 9: **end for**
- 10: **return** Ex

Setup (hypergraph, per-local instance). Let $H = (V, \mathcal{E})$ be a hypergraph and write $r := \max_{S \in \mathcal{E}} |S|$ for its (global) maximum hyperedge size. For each hyperedge $S \in \mathcal{E}$, let $H_S := H_p(S)$. Write $n_S := |V(H_S)|$, $A_S := \sum_{T \in \mathcal{E}(H_S)} |T|$ for the total arity within H_S , and let $t_S := \text{tw}(PG(H_S))$ be the treewidth of the primal graph. Let w_S denote the TD width actually used by the DP on H_S , and set $L := 2p + 1$. Define the global aggregates

$$N_H := \sum_{S \in \mathcal{E}} n_S, \quad A_H := \sum_{S \in \mathcal{E}} A_S, \quad t := \max_S t_S, \quad \kappa := \max_S w_S.$$

We use the unit-cost RAM model; per-round trigonometric coefficients are pretabulated (affecting only polynomial factors).

Tree decomposition on $PG(H_S)$. Using any single-exponential 2-approximation for treewidth, we obtain a TD for $PG(H_S)$ of width $w_S \leq 2t_S + 1$ in time

$$T_{\text{TD}}(H_S) = \tilde{O}(n_S \cdot 2^{O(t_S)}).$$

Per-local DP on H_S . Each bag of $PG(H_S)$ contains at most $w_S + 1$ vertices and thus has $2^{L(w_S+1)}$ replicated-spin assignments. Aggregating local kernels/phases and child messages per assignment gives

$$T_{\text{DP}}(H_S) = 2^{L(w_S+1)} \cdot \tilde{O}(n_S + A_S), \quad S_{\text{DP}}(H_S) = 2^{L(w_S+1)} \cdot \tilde{O}(n_S),$$

where $\tilde{O}(\cdot)$ hides factors polynomial in p, w_S, r and the input size of H_S .

Global cost (sum over local p -instances). Extracting each H_S on $PG(H)$ costs $\tilde{O}(n_S + A_S)$, hence $\sum_S \tilde{O}(n_S + A_S) = \tilde{O}(N_H + A_H)$. Summing the TD and DP costs over $S \in \mathcal{E}$ and using $t = \max_S t_S$ and $\kappa = \max_S w_S$ yields

$$T_{\text{total}}^{(\text{hyper})} \leq \underbrace{\tilde{O}(N_H + A_H)}_{\text{extract all } H_S} + \underbrace{\tilde{O}(N_H \cdot 2^{O(t)})}_{\text{TD 2-approx on } PG(H_S)} + \underbrace{2^{L(\kappa+1)} \cdot \tilde{O}(N_H + A_H)}_{\text{all bag-level DP}}. \quad (4.14)$$

In particular (for fixed p), the DP term dominates asymptotically:

$$T_{\text{total}}^{(\text{hyper})} = 2^{L(\kappa+1)} \cdot \tilde{O}(N_H + A_H) + (\text{lower-order terms}), \quad S_{\text{total}}^{(\text{hyper})} = 2^{L(\kappa+1)} \cdot \tilde{O}(N_H),$$

where the space bound follows by processing the H_S sequentially and freeing temporaries after each subproblem.

Bounded local treewidth on $PG(H_S)$ (fixed p). If $\max_S t_S = O(1)$, then also $\kappa = O(1)$ for the 2-approx TD (and $\kappa = t$ with exact TDs), whence

$$T_{\text{total}}^{(\text{hyper})} = \text{poly}(N_H + A_H), \quad S_{\text{total}}^{(\text{hyper})} = \text{poly}(N_H).$$

With exact TDs the DP factor tightens from $2^{L(\kappa+1)}$ to $2^{L(t+1)}$.

5 Experiments

We conduct fixed-round QAOA experiments on three classes of structured graphs (see Fig. 2) using the exact p -local expectation evaluator proposed in Sec. 4. Using the normalized cut ratio $\langle C \rangle / |E|$ as the metric, we compare constant-round performance across these graphs, which differ in their short-cycle density and local geometry, and include classical baselines that are *locality-matched* to QAOA for a fair comparison¹.

5.1 Graph Families and Rationale

Generalized Petersen graph $GP(15, 2)$. The generalized Petersen graphs $GP(n, k)$ form a well-studied family [26]; here we use $GP(15, 2)$, a canonical benchmark on 30 vertices and 45 edges (in particular 3-regular), built from an outer 15-cycle, an inner 15-cycle connected with step 2, and 15 radial spokes. Formally (indices modulo 15), the edge sets are $\{v_i, v_{i+1}\}$, $\{v_i, w_i\}$, and $\{w_i, w_{i+2}\}$ for $i = 0, \dots, 14$. This construction injects a controlled supply of short odd cycles so the graph is non-bipartite with girth 5. The dihedral symmetries (rotations/reflections of the index i) keep local neighborhoods essentially uniform, enabling controlled studies of short-cycle effects at fixed degree.

Double-layer triangular lattice via iterated 2-lifts. We view this graph as a simple example of an iterated 2-lift of a triangular base graph in the sense of Bilu and Linial [27]. Iterated 2-lifts provide a scalable construction with highly regular local neighborhoods and abundant short cycles. The uniform local structure enables like-for-like comparisons between QAOA and classical local rules under the same protocol.

Truncated icosahedron graph C_{60} . C_{60} is the truncated icosahedron graph of the truncated icosahedron, a 3-regular fullerene formed by a pentagon–hexagon tiling with two edge types. Its girth is 5, and the pentagonal faces introduce unavoidable local frustration for the Max-Cut objective. The high symmetry distributes this frustration uniformly across the graph, making C_{60} a demanding test case for purely k -local classical rules; geometrically, it is the familiar truncated icosahedron / fullerene polyhedron [28]. Meanwhile, the bounded degree and homogeneous local neighborhoods resemble nearest-neighbor quantum hardware layouts. For our evaluator, every edge-radius-3 neighborhood has treewidth 3, so a p -local dynamic-programming scheme can exactly compute expectation values at shallow p . These features make C_{60} a physically meaningful, symmetry-rich stress test on which shallow QAOA can be probed against challenging classical baselines.

5.2 Evaluation Protocol and Classical Baselines

Metric and evaluator. We report the normalized expected cut fraction $\langle C \rangle / |E|$. Expectations at fixed round p are computed exactly using a p -local evaluator: for each edge, we assemble the contribution from its radius- p neighborhood via tree-decomposition DP and sum over edges.

¹Source code and instructions are available at https://github.com/WABINSH/QAOA_expectation_experiment.git.

Table 1: p -local treewidth for the three instances.

Instance	$p = 1$	$p = 2$	$p = 3$
$GP(15, 2)$	1	2	3
Double-layer triangular 2-lift	2	2	2
C_{60}	1	2	3

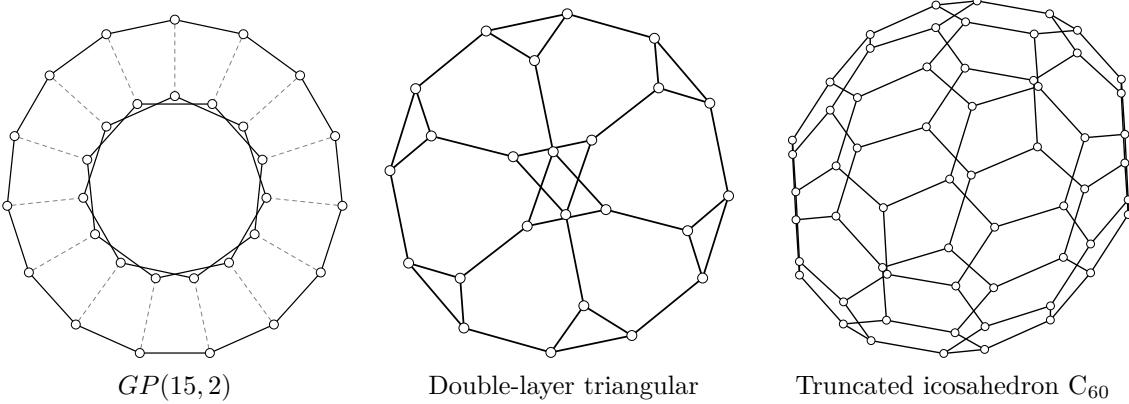


Figure 2: Three structured graph benchmarks.

Our complexity bounds in Sec. 4 rely on the near-linear-time 2-approximation algorithm for treewidth [25]. In the experiments of Sec. 5, however, we instead use a simple branch-and-bound treewidth routine to construct tree decompositions, since our benchmark graphs are small. This choice only affects preprocessing time and does not change any of the reported expectations.

Classical locality-matched baselines. To match the p -local lightcone of QAOA, we fix the locality budget at $k = p$ and compare two representative families. For each instance and each p , we tune the family-specific parameters and report the larger expected cut fraction as the “best classical local” reference. Both families are label-invariant and access only radius- k neighborhoods.

(i) *Threshold-flip Th- $s(\tau)$* [29]. Starting from i.i.d. unbiased Rademacher spins $\sigma^{(0)} \in \{\pm 1\}^V$,

$$\Pr[\sigma_v^{(0)} = +1] = \Pr[\sigma_v^{(0)} = -1] = \frac{1}{2} \quad \text{for all } v \in V,$$

we perform s synchronous rounds. In the abstract Th- $s(\tau)$ family one may parameterize round- t thresholds by fractions $\tau_t \in [0, 1]$ and set

$$\sigma_v^{(t+1)} = \begin{cases} -\sigma_v^{(t)}, & \text{if } \#\{u \in N(v) : \sigma_u^{(t)} = \sigma_v^{(t)}\} \geq \theta_v^{(t)}, \\ \sigma_v^{(t)}, & \text{otherwise,} \end{cases} \quad \theta_v^{(t)} = \lceil \tau_t d_v \rceil,$$

so that a flip is triggered once a large enough fraction τ_t of the neighbors agree with $\sigma_v^{(t)}$. After s rounds, the final assignment $\sigma^{(s)}$ induces the cut. This rule is s -local (information cannot propagate beyond s hops), so we instantiate it with $s \leq k = p$.

In our experiments we use a discrete variant tailored to the small, bounded-degree benchmark graphs. Instead of optimizing over all $\tau_t \in [0, 1]$, we work directly with integer thresholds shared by all vertices in a round: for each round t we pick an integer $t_t \in \{1, 2, 3\}$ and use

$$\theta_v^{(t)} = t_t \quad \text{for all } v \in V.$$

Equivalently, this corresponds to restricting τ_t to a coarse grid that depends on the degree, $\tau_t \approx t_t/d_v$. For each graph and each round p , we search over $s \in \{1, \dots, p\}$ and all sequences

$(t_t)_{t=0}^{s-1}$ with entries in $\{1, 2, 3\}$. For every candidate choice we approximate the expected cut fraction by Monte Carlo, averaging the cut ratio over $T = 5000$ independent draws of the unbiased initial spins.

(ii) *Barak–Marwaha-type BM- k Gaussian-sum rule* [30]. Sample i.i.d. seeds $g_u \sim \mathcal{N}(0, 1)$ for all $u \in V$. For each vertex v , compute a radius- k linear score with distance-dependent weights $\alpha = (\alpha_0, \dots, \alpha_k)$:

$$S_v(\alpha, g) = \sum_{d=0}^k \alpha_d \sum_{\substack{u \in V: \\ \text{dist}(u, v) = d}} g_u, \quad \sigma_v = \text{sign}(S_v(\alpha, g)),$$

with the convention $\text{sign}(0) = +1$. This is a one-shot radius- k local rule; we take $k = p$ and optimize α up to an overall scale (which does not affect the signs). For convenience we fix $\alpha_0 = 1$ and optimize the remaining coordinates by a small black-box search (random restarts followed by simple coordinate-wise refinement). Because the scores $\{S_v(\alpha, g)\}$ are jointly Gaussian, the expected cut fraction can be evaluated exactly using the identity $\Pr[\text{sign}(X) \neq \text{sign}(Y)] = \arccos(\rho)/\pi$ for jointly Gaussian X, Y with correlation ρ , rather than by sampling the seeds g .

Protocol. For each graph and round p , we (a) fix $k = p$; (b) independently tune $(s, (t_t)_{t=0}^{s-1})$ for Th- $s(\tau)$ and α for BM- k within the ranges described above; (c) evaluate each family’s expected cut fraction (exactly for BM- k and by Monte Carlo for Th- s); and (d) take their pointwise maximum as the “best classical local” baseline. The optimized baseline parameters are summarized in Tabs. 2 and 3, and the resulting cut fractions appear in Tabs. 4, 5, and 6.

Table 2: BM- k parameter settings for Sec. 5.

p	Instance	BM- k params α
1	$GP(15, 2)$	$\{1, -0.5770\}$
1	Double-layer triangular 2-lift	$\{1, -0.4800\}$
1	Truncated icosahedron C_{60}	$\{1, -0.5779\}$
2	$GP(15, 2)$	$\{1, -0.7021, 0.2391\}$
2	Double-layer triangular 2-lift	$\{1, -0.5932, 0.2842\}$
2	Truncated icosahedron C_{60}	$\{1, -0.7255, 0.2897\}$
3	$GP(15, 2)$	$\{1, -0.7209, 0.2793, -0.0973\}$
3	Double-layer triangular 2-lift	$\{1, -0.6428, 0.4050, -0.1638\}$
3	Truncated icosahedron C_{60}	$\{1, -0.7864, 0.4270, -0.2092\}$

Table 3: Th- s parameter settings for Sec. 5.

p	Instance	Th- s thresholds $(t_t)_{t=0}^{s-1}$
1	$GP(15, 2)$	$\{3\}$
1	Double-layer triangular 2-lift	$\{3\}$
1	Truncated icosahedron C_{60}	$\{3\}$
2	$GP(15, 2)$	$\{2, 3\}$
2	Double-layer triangular 2-lift	$\{3, 3\}$
2	Truncated icosahedron C_{60}	$\{2, 3\}$
3	$GP(15, 2)$	$\{3, 2, 3\}$
3	Double-layer triangular 2-lift	$\{2, 3, 3\}$
3	Truncated icosahedron C_{60}	$\{3, 2, 3\}$

Table 4: QAOA and classical local baselines on $GP(15, 2)$ ($n = 30, m = 45$).

p	γ	β	QAOA	BM- k	Th- s
1	{0.3077}	{0.3927}	0.6624	0.6959	0.6882
2	{0.2437, 0.4431}	{0.5159, 0.2513}	0.7360	0.7477	0.7021
3	{0.2110, 0.3990, 0.4685}	{0.6090, 0.4590, 0.2350}	0.7836	0.7561	0.7589

Table 5: QAOA and classical local baselines on the double-layer triangular 2-lift ($n = 24, m = 36$).

p	γ	β	QAOA	BM- k	Th- s
1	{0.2851}	{0.3481}	0.6599	0.6587	0.6448
2	{0.2917, 0.5623}	{0.4090, 0.2408}	0.7208	0.6964	0.6578
3	{0.2014, 0.4855, 0.5916}	{0.5410, 0.3187, 0.1851}	0.7456	0.7114	0.7145

Table 6: QAOA and classical local baselines on the truncated icosahedron graph C_{60} ($n = 60, m = 90$).

p	γ	β	QAOA	BM- k	Th- s
1	{0.3078}	{0.3927}	0.6925	0.6959	0.6870
2	{0.2490, 0.4451}	{0.5252, 0.2469}	0.7514	0.7584	0.7297
3	{0.2110, 0.3990, 0.4685}	{0.6090, 0.4590, 0.2350}	0.7893	0.7868	0.7801

5.3 Synthesis

Tabs 4, 5, and 6, together with Fig. 3, point to three nontrivial features across the generalized Petersen graph $GP(15, 2)$, the double-layer triangular 2-lift, and the truncated icosahedron graph C_{60} . Note that for $p = 3$ we did not perform exhaustive per-instance angle optimization; instead we used heuristic schedules for 3-regular graphs proposed in [31] as our initial choices and applied only mild tuning. Even with this deliberately non-optimized choice, QAOA already exceeds the locality-matched classical baselines (Tabs 4, 5, 6; Fig. 3).

Matched-locality gap depends on the family. When QAOA at round p is compared with classical k -local baselines at matched lightcone radius ($k \approx p$), both the sign and magnitude of the quantum-classical gap vary markedly by graph family. On the double-layer triangular 2-lift, QAOA shows a consistent advantage already at $p \leq 3$ (cf. Tab 5).

Crossover depth on $GP(15, 2)$. On $GP(15, 2)$, classical p -local rules are competitive at very small p , whereas QAOA overtakes at a moderate depth (see Tab. 4 and Fig. 3). At depth $p = 1$, both Th- $s(\tau)$ and BM- k achieve slightly higher cut fractions than QAOA under the matched locality budget $k = p$. By $p = 2$, QAOA already surpasses the threshold-flip baseline, although BM- k still attains the best cut fraction. At $p = 3$, even with only mildly tuned angles, QAOA yields the highest cut fraction among all tested methods on this instance. This behaviour exhibits a genuine crossover in the constant-round regime: very local classical rules can match or slightly outperform depth-one QAOA, but shallow QAOA gains a clear advantage once a few layers are allowed while still remaining in the constant-round regime.

Emergent advantage on C_{60} . On the truncated icosahedron C_{60} (3-regular, girth 5), QAOA surpasses the best matched-local classical baselines once the depth reaches a modest threshold: by $p = 3$, QAOA yields the highest cut fraction among all $k \approx p$ methods under our exact, lightcone-matched evaluation protocol (cf. Tab 6). The absolute margins are small, but the direction is consistent with a depth requirement for coordinating phases across the pentagon–hexagon tiling and resolving local frustration that strictly k -local updates cannot capture at shallower radii. In short, on C_{60} we observe a numerical crossover at moderate depth: classical locality remains competitive in value, yet the best performance is achieved by QAOA once the problem-dependent depth threshold is cleared, aligning with the crossover pattern observed on $GP(15, 2)$.

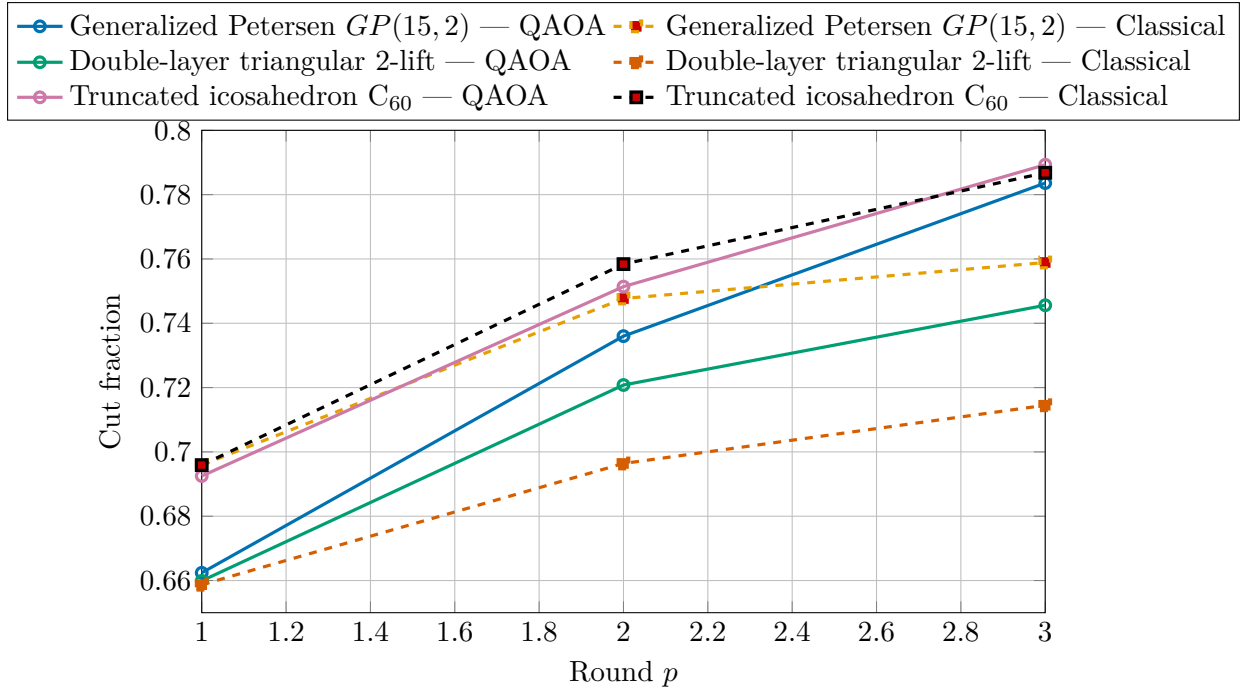


Figure 3: Cut fraction versus QAOA round p on three graph families (solid: QAOA; dashed: best classical local).

6 Conclusions

We provided a complexity-algorithm account of exact expectation evaluation for fixed-round QAOA. On the complexity side, for Max-Cut and round $p \geq 2$, we proved NP-hardness of exact evaluation and, further, NP-hardness under $2^{-O(n)}$ additive error; on the algorithmic side, we designed a bag-level dynamic program over p -lightcone neighborhoods whose running time is polynomial in the input size and singly-exponential in a local width parameter (the p -local treewidth), enabling exact evaluation on families with (hyper)local width growing at most logarithmically. Using a p -local evaluator, we benchmarked against locality-matched classical baselines on $GP(15, 2)$, a double-layer triangular 2-lift, and C_60 . We observe modest gaps at shallow p on the triangular 2-lift, a $GP(15, 2)$ crossover with QAOA ahead at $p=3$, and a small $p=3$ advantage on C_60 (3-regular, girth 5). These effects are instance-dependent and limited to the tested rounds.

In the future, we will further conduct in-depth research on the following issues: (i) *Rounds under bounded degree*. For bounded-degree graphs at rounds $p = \Theta(\log n)$, either design a polynomial time procedure that evaluates the QAOA expected cut, or show that no such polynomial-time evaluation exists. (ii) *Beyond the standard mixer*. Quantify how alternative mixers (e.g., XY , constraint-preserving) and generalized alternating-operator families affect additive/relative-error hardness, and integrate exact p -local evaluation with structure-aware parameter search to provide reproducible tuning baselines.

Acknowledgements

This work was supported in part by the Quantum Science and Technology-National Science and Technology Major Project under Grant No. 2024ZD0300500 and the National Natural Science Foundation of China Grants No. 62325210, 62272441, 12501450.

References

- [1] Edward Farhi, Jeffrey Goldstone, and Sam Gutmann. “A quantum approximate optimization algorithm” (2014). [arXiv:1411.4028](https://arxiv.org/abs/1411.4028).
- [2] Stuart Hadfield, Zhihui Wang, Bryan O’Gorman, et al. “From the quantum approximate optimization algorithm to a quantum alternating operator ansatz”. *Algorithms* **12**, 34 (2019).
- [3] Leo Zhou, Sheng-Tao Wang, Soonwon Choi, Hannes Pichler, and Mikhail D. Lukin. “Quantum approximate optimization algorithm: Performance, mechanism, and implementation on near-term devices”. *Physical Review X* **10**, 021067 (2020).
- [4] Kostas Blekos, Dean Brand, Andrea Ceschini, Chiao-Hui Chou, Rui-Hao Li, Komal Pandya, and Alessandro Summer. “A review on quantum approximate optimization algorithm and its variants”. *Physics Reports* **1068**, 1–66 (2024).
- [5] Daniel J. Egger, Jakub Mareček, and Stefan Woerner. “Warm-starting quantum optimization”. *Quantum* **5**, 479 (2021).
- [6] Ryan Tate, Jay Moondra, Bryan Gard, Greg Mohler, and Swati Gupta. “Warm-started QAOA with custom mixers provably converges and computationally beats Goemans–Williamson’s Max-Cut at low circuit depths”. *Quantum* **7**, 1121 (2023).
- [7] Stefan H. Sack and Maksym Serbyn. “Quantum annealing initialization of the quantum approximate optimization algorithm”. *Quantum* **5**, 491 (2021).
- [8] Luning Zhu, Ho Lun Tang, George S. Barron, Fernando A. Calderon-Vargas, Nicholas J. Mayhall, Edwin Barnes, and Sophia E. Economou. “Adaptive quantum approximate optimization algorithm for solving combinatorial problems on a quantum computer”. *Physical Review Research* **4**, 033029 (2022).
- [9] Pranav Chandarana, Nayana N. Hegade, Kankana Paul, Fredy Albarrán-Arriagada, Enrique Solano, Adolfo del Campo, and Xi Chen. “Digitized-counterdiabatic quantum approximate optimization algorithm”. *Physical Review Research* **4**, 013141 (2022).
- [10] Sai Hari Sureshbabu, Daniel Herman, Ruslan Shaydulin, Jacopo Basso, Shouvanik Chakrabarti, Yao Sun, and Marco Pistoia. “Parameter setting in quantum approximate optimization of weighted problems”. *Quantum* **8**, 1231 (2024).
- [11] Jakob Weidenfeller, Luis C. Valor, Julien Gacon, Christian Tornow, Lucas Bello, Daniel J. Egger, and Stefan Woerner. “Scaling of the quantum approximate optimization algorithm on superconducting qubit-based hardware”. *Quantum* **6**, 870 (2022).
- [12] Jonathan Wurtz and Peter J. Love. “MaxCut quantum approximate optimization algorithm performance guarantees for $p > 1$ ”. *Physical Review A* **103**, 042612 (2021).
- [13] Joao Basso, David Gamarnik, Song Mei, and Leo Zhou. “Performance and limitations of the QAOA at constant levels on large sparse hypergraphs and spin glass models”. In 2022 IEEE 63rd Annual Symposium on Foundations of Computer Science (FOCS). Pages 335–343. (2022). [arXiv:2204.10306](https://arxiv.org/abs/2204.10306).
- [14] Jacopo Basso, Edward Farhi, Kushagra Marwaha, Benjamin Villalonga, and Leo Zhou. “The QAOA at high depth for MaxCut on large-girth regular graphs and the SK model”. In Proceedings of TQC 2022. Volume 232 of LIPIcs, pages 7:1–7:21. (2022).
- [15] Kushagra Marwaha. “Local classical Max-Cut algorithm outperforms $p=2$ QAOA on high-girth regular graphs”. *Quantum* **5**, 437 (2021).
- [16] Matthew B. Hastings. “Classical and quantum bounded depth approximation algorithms”. *Quantum Information and Computation* **19**, 1116–1140 (2019).

[17] Tongyang Li, Yiming Su, Zhen Yang, and Shengyu Zhang. “Quantum approximate optimization algorithms for maximum cut on low-girth graphs”. *Physical Review Research* **7**, 033014 (2025).

[18] David Eppstein. “Diameter and treewidth in minor-closed graph families”. *Algorithmica* **27**, 275–291 (2000).

[19] Erik D. Demaine and Mohammad Taghi Hajiaghayi. “Equivalence of local treewidth and linear local treewidth and its algorithmic applications”. In Proceedings of the ACM-SIAM Symposium on Discrete Algorithms (SODA). Pages 840–849. SIAM (2004). url: <https://dl.acm.org/doi/10.5555/982792.982919>.

[20] Erik D. Demaine, Fedor V. Fomin, Mohammad Taghi Hajiaghayi, and Dimitrios M. Thilikos. “Subexponential parameterized algorithms on graphs of bounded genus and h -minor-free graphs”. *Journal of the ACM* **52**, 866–893 (2005).

[21] Sang-il Oum and Paul D. Seymour. “Approximating clique-width and branch-width”. *Journal of Combinatorial Theory, Series B* **96**, 514–528 (2006).

[22] Edward Farhi and Aram W. Harrow. “Quantum supremacy through the quantum approximate optimization algorithm” (2016). [arXiv:1602.07674](https://arxiv.org/abs/1602.07674).

[23] Hari Krovi. “Average-case hardness of estimating probabilities of random quantum circuits with a linear scaling in the error exponent” (2022). [arXiv:2206.05642](https://arxiv.org/abs/2206.05642).

[24] H. L. Bodlaender. “A linear-time algorithm for finding tree-decompositions of small treewidth”. *SIAM Journal on Computing* **25**, 1305–1317 (1996).

[25] Tuukka Korhonen. “A single-exponential time 2-approximation algorithm for treewidth”. *SIAM Journal on Computing* (2023).

[26] Roberto Frucht, Jack E. Graver, and Mark E. Watkins. “The groups of the generalized Petersen graphs”. *Mathematical Proceedings of the Cambridge Philosophical Society* **70**, 211–218 (1971).

[27] Yonatan Bilu and Nathan Linial. “Lifts, discrepancy and nearly optimal spectral gap”. *Combinatorica* **26**, 495–519 (2006).

[28] Bertram Kostant. “Structure of the truncated icosahedron (such as fullerene or viral coatings) and a 60-element conjugacy class in $PSL(2, 11)$ ”. *Proceedings of the National Academy of Sciences of the USA* **91**, 11714–11717 (1994).

[29] Juho Hirvonen, Joel Rybicki, Stefan Schmid, and Jukka Suomela. “Large cuts with local algorithms on triangle-free graphs” (2014). [arXiv:1402.2543](https://arxiv.org/abs/1402.2543).

[30] Boaz Barak and Kunal Marwaha. “Classical algorithms and quantum limitations for maximum cut on high-girth graphs” (2021). [arXiv:2106.05900](https://arxiv.org/abs/2106.05900).

[31] Jonathan Wurtz and Denis Lykov. “Fixed-angle conjectures for the quantum approximate optimization algorithm on regular MaxCut graphs”. *Physical Review A* **104**, 052419 (2021).

A Recovering MAXCUT(G) from MAXCUT(G')

This appendix proves that, for the graph $G' = (V', E')$ obtained by the four-step construction in Sec. 3, one can recover in polynomial time the maximum cut of the original graph $G = (V, E)$ from any maximum cut of G' . Recall that the construction consists of the following four components:

1. **Vertex gadgets.** For every $u \in V(G)$, replace u by a complete bipartite graph $B(u) \cong K_{n_0+1, 10n_0}$ with (L_u, R_u) , where $|L_u| = n_0 + 1$ and $|R_u| = 10n_0$.
2. **Synchronous edges.** For every original edge $(u, v) \in E(G)$ and each pair $u_{1,i} \in L_u, v_{1,i} \in L_v$ with $\forall i \in \{0, 1, \dots, n_0\}$, add an edge $\{u_{1,i}, v_{1,i}\}$.
3. **Global bipartite frame.** Add the bipartite graph $K_{100n_0^2, 100n_0^2} = (X, Y)$ with $|X| = |Y| = 100n_0^2 := M$ and connect the special vertices $x_0 \in X$ and $y_0 \in Y$ to all gadget vertices.
4. **Anchor and control edges.** Add a vertex w and connect it to x_0, y_0 , and every $u_{1,0}$; in total this gives $n_0 + 2$ edges.

To show that MAXCUT(G) can be recovered from MAXCUT(G') in polynomial time, we first prove three lemmas.

Lemma A.1. *(The global frame must be cut as a whole) In any maximum cut*

$$(S', V' \setminus S')$$

of G' , the two sides of the global bipartite frame must fall into opposite parts of the cut:

$$X \subseteq S', Y \subseteq V' \setminus S' \quad \text{or} \quad Y \subseteq S', X \subseteq V' \setminus S'.$$

Proof. Let $X' := X \setminus \{x_0\}, Y' := Y \setminus \{y_0\}$, so that

$$|X'| = |Y'| = M - 1 = 100n_0^2 - 1.$$

By construction, except for x_0, y_0 , vertices in X', Y' have no edges going outside the frame; all outside edges are concentrated on x_0, y_0 .

Case (1): x_0 and y_0 are on opposite sides. If we put all of X on the side of x_0 and all of Y on the side of y_0 , then all M^2 edges of $K_{M,M}$ are cut. In addition, x_0, y_0 cut their external edges in total $n_0(11n_0 + 1) + 1$ edges. Hence, in this case, we obtain

$$M^2 + n_0(11n_0 + 1) + 1. \tag{A.1}$$

Case (2): x_0 and y_0 are on the same side. Assume they are both in $V' \setminus S'$. Write

$$a := |X' \cap S'|, \quad b := |X' \setminus S'| = (M - 1) - a,$$

$$c := |Y' \cap S'|, \quad d := |Y' \setminus S'| = (M - 1) - c.$$

The cut edges inside the frame consist of:

1. edges in $X' \times Y'$: they contribute $ad + bc$;
2. edges from x_0 to $Y' \cap S'$: they contribute c ;
3. edges from y_0 to $X' \cap S'$: they contribute a .

Together with at most $2n_0(11n_0 + 1) + 2$ external cut edges, we get

$$f(a, c) \leq ad + bc + a + c + 2n_0(11n_0 + 1) + 2.$$

Substituting $b = (M - 1) - a$ and $d = (M - 1) - c$ gives

$$\begin{aligned} f(a, c) &\leq a((M - 1) - c) + ((M - 1) - a)c + a + c + 2n_0(11n_0 + 1) + 2 \\ &= (M - 1)(a + c) - 2ac + a + c + 2n_0(11n_0 + 1) + 2 \\ &= M(a + c) - 2ac + 2n_0(11n_0 + 1) + 2. \end{aligned} \quad (\text{A.2})$$

Because of the negative term $-2ac$, the maximum is obtained on the boundary; taking $a = 0$ we have

$$f(0, c) \leq Mc + 2n_0(11n_0 + 1) + 2 \leq (M - 1)M + 2n_0(11n_0 + 1) + 2. \quad (\text{A.3})$$

Comparing (A.1) and (A.3), and using $M = 100n_0^2$, we obtain

$$(M^2 + n_0(11n_0 + 1) + 1) - ((M - 1)M + 2n_0(11n_0 + 1) + 2) = M - n_0(11n_0 + 1) - 1 = 89n_0^2 - n_0 - 1 > 0.$$

Thus every arrangement with x_0, y_0 on the same side yields a strictly smaller cut than putting the whole frame on opposite sides. By maximality only Case (1) can occur. \square

Lemma A.2. (*Gadget bipartition is separated*) *For every $u \in V(G)$, let $B(u) \cong K_{n_0+1, 10n_0}$ be its gadget with bipartition (L_u, R_u) , where $|L_u| = n_0 + 1$ and $|R_u| = 10n_0$. In any maximum cut*

$$(S', V' \setminus S')$$

of G' , the gadget $B(u)$ is separated along this bipartition, i.e.

$$L_u \subseteq S', R_u \subseteq V' \setminus S' \quad \text{or} \quad R_u \subseteq S', L_u \subseteq V' \setminus S'.$$

Proof. Fix any original vertex $u \in V(G)$ and its gadget $B(u)$. By Lemma A.1, in any maximum cut of G' the special vertices x_0 and y_0 lie on opposite sides of the cut. Moreover, by construction every vertex of every gadget $B(u)$ is adjacent to both x_0 and y_0 . Therefore, for each vertex $v \in B(u)$, exactly one of the edges $\{v, x_0\}$ and $\{v, y_0\}$ is cut, regardless of which side of the cut v lies on. In particular, if we compare two cuts that differ only in the placement of vertices inside $B(u)$, then the total contribution of all edges between $B(u)$ and $\{x_0, y_0\}$ to the cut size is the same. Hence, when reasoning about local modifications inside $B(u)$, we may ignore edges from $B(u)$ to $\{x_0, y_0\}$ and only track edges inside $B(u)$ and the remaining external edges of $B(u)$.

By the construction of synchronous and anchor edges, each vertex in L_u is adjacent to all $10n_0$ vertices of R_u and to at most $n_0 + 2$ vertices outside $B(u)$. Vertices in R_u are adjacent only to L_u (besides x_0, y_0 , which we ignore as argued above).

Step 1: in any maximum cut all of L_u lie on the same side. Suppose for contradiction that there exists a maximum cut $(S_0, V' \setminus S_0)$ of G' such that L_u is split between the two sides. Write

$$a := |L_u \cap S_0|, \quad b := |L_u \cap (V' \setminus S_0)|,$$

and assume without loss of generality that $a \geq b \geq 1$.

First, we move all vertices of R_u to the side $V' \setminus S_0$ without decreasing the cut. Indeed, consider any $r \in R_u \cap S_0$. The edges from r to L_u contribute b cut edges before the move (those to $L_u \cap (V' \setminus S_0)$), and a cut edges after we move r to $V' \setminus S_0$ (those to $L_u \cap S_0$). Since $a \geq b$ and r has no neighbours outside $B(u)$ other than x_0, y_0 , the cut size does not decrease. Performing this operation for all $r \in R_u \cap S_0$ yields a maximum cut $(S_1, V' \setminus S_1)$ with

$$R_u \subseteq V' \setminus S_1$$

and still L_u split between the two sides.

Now consider any vertex $\ell \in L_u \cap (V' \setminus S_1)$. Since $B(u)$ is complete bipartite between L_u and R_u and $R_u \subseteq V' \setminus S_1$, ℓ has all $10n_0$ neighbours in R_u on the same side as itself. If we move ℓ from $V' \setminus S_1$ to S_1 , then:

- all $10n_0$ edges from ℓ to R_u become cut edges (they were not cut before);
- at most $n_0 + 2$ external edges from ℓ to vertices outside $B(u)$ may change from cut to non-cut in the worst case.

Thus the net change in the cut size is at least

$$10n_0 - (n_0 + 2) = 9n_0 - 2 > 0$$

for every integer $n_0 \geq 1$, contradicting the maximality of $(S_0, V' \setminus S_0)$. Therefore, in any maximum cut, all vertices in L_u must lie on the same side.

Step 2: in any maximum cut all of R_u lie on the opposite side. Let $(S_2, V' \setminus S_2)$ be a maximum cut. By Step 1, all vertices in L_u lie on the same side; without loss of generality we assume

$$L_u \subseteq S_2.$$

Suppose, for contradiction, that R_u is not contained in a single side. Then there exists some $q \in R_u \cap S_2$. Recall that, besides x_0, y_0 , the vertex q has no neighbours outside $B(u)$; and as argued at the beginning of the proof, edges to x_0, y_0 can be ignored when comparing cuts that differ only on $B(u)$.

Before moving q , all its neighbours in L_u lie in S_2 , so none of the $|L_u| = n_0 + 1$ edges from q to L_u are cut. If we move q from S_2 to $V' \setminus S_2$, then all these $n_0 + 1$ edges become cut edges, and we do not lose any cut edges incident to q outside $B(u)$. Therefore the cut size strictly increases by at least $n_0 + 1 > 0$, contradicting the maximality of $(S_2, V' \setminus S_2)$. Hence R_u cannot be split: in every maximum cut all vertices in R_u lie on the side opposite to L_u .

Combining Steps 1 and 2, we conclude that in any maximum cut of G' the gadget $B(u)$ is separated along its bipartition (L_u, R_u) , as claimed. \square

Lemma A.3. *(Projection of a maximum cut is a maximum cut of G)*

Let $(S', V' \setminus S')$ be any maximum cut of G' . Define $S := \{u \in V(G) \mid L_u \subseteq S'\}$. Then $(S, V(G) \setminus S)$ is a maximum cut of the original graph G .

Proof. By Lemma A.2, in every maximum cut of G' each gadget $B(u)$ has its two parts entirely on opposite sides, so the above definition is well-defined: for each u exactly one of L_u, R_u is contained in S' .

For every original edge $(u, v) \in E(G)$, the construction adds $n_0 + 1$ synchronous edges $\{u_{1,0}, v_{1,0}\}, \dots, \{u_{1,n_0}, v_{1,n_0}\}$, with endpoints in L_u and L_v , respectively. If by the above definition $u \in S$ and $v \notin S$, then all these $n_0 + 1$ edges are cut; if u, v fall on the same side, none of them is cut. Hence the contribution of synchronous edges to the cut value of G' is exactly $(n_0 + 1) \cdot \text{cut}_G(S)$.

On the other hand, by Lemma A.1 and Lemma A.2 the internal cut value of the frame $K_{100n_0^2, 100n_0^2}$ and of every gadget $B(u)$ is already fixed at its maximum. The frame contributes $M^2 + n_0(11n_0 + 1) + 1$, and each gadget, when separated, contributes $(n_0 + 1) \cdot 10n_0$. There are n_0 gadgets, so altogether they contribute $10n_0^2(n_0 + 1)$. These parts are independent of S and can be grouped into an explicit polynomial in n_0 :

$$b(n_0) := (10000n_0^4 + n_0(11n_0 + 1) + 1) + 10n_0^2(n_0 + 1).$$

There remain at most n_0 “variable” edges incident to the anchor w ; collect their total contribution into a remainder $r(S, n_0)$, where $0 \leq r(S, n_0) \leq n_0$. Thus for the maximum cut $(S', V' \setminus S')$ we have

$$\text{cut}_{G'}(S', V' \setminus S') = b(n_0) + (n_0 + 1) \cdot \text{cut}_G(S) + r(S, n_0), \quad 0 \leq r(S, n_0) \leq n_0. \quad (\text{A.4})$$

Let $S^* \subseteq V(G)$ be an actual maximum cut of G , so that $\text{cut}_G(S^*) = \text{MAXCUT}(G)$. If we carry out the above construction according to S^* , we obtain a cut of G' of value

$$b(n_0) + (n_0 + 1) \cdot \text{MAXCUT}(G) + r(S^*, n_0). \quad (\text{A.5})$$

Since $(S', V' \setminus S')$ is a *maximum* cut of G' , comparing (A.4) and (A.5) yields

$$b(n_0) + (n_0 + 1) \cdot \text{cut}_G(S) + r(S, n_0) \geq b(n_0) + (n_0 + 1) \cdot \text{MAXCUT}(G) + r(S^*, n_0).$$

Because $0 \leq r(S, n_0), r(S^*, n_0) \leq n_0$, the above forces $\text{cut}_G(S) \geq \text{MAXCUT}(G)$, and hence equality must hold: $\text{cut}_G(S) = \text{MAXCUT}(G)$. \square

Polynomial-time recovery

From (A.4) we have

$$\text{MAXCUT}(G') = b(n_0) + (n_0 + 1) \cdot \text{MAXCUT}(G) + r(S, n_0), \quad 0 \leq r(S, n_0) \leq n_0. \quad (\text{A.6})$$

Since $b(n_0) = (10000n_0^4 + n_0(11n_0 + 1) + 1) + 10n_0^2(n_0 + 1)$ is explicit and depends only on the construction, we can recover $\text{MAXCUT}(G)$ from $\text{MAXCUT}(G')$ by

$$\text{MAXCUT}(G) = \left\lfloor \frac{\text{MAXCUT}(G') - b(n_0)}{n_0 + 1} \right\rfloor. \quad (\text{A.7})$$

This involves only a constant number of arithmetic operations and is clearly polynomial time. Hence, from any maximum cut of G' we can recover $\text{MAXCUT}(G)$ in polynomial time.

B From Complete-Basis Insertions to the Master Formula

Inspired by [14], we derive a compact “master formula” for two-point observables under fixed-round QAOA that separates on-site mixer amplitudes from two-site cost phases and makes p -locality explicit.

Setup. Let

$$|\psi_p(\boldsymbol{\gamma}, \boldsymbol{\beta})\rangle = \left(\prod_{\ell=1}^p e^{-i\beta_\ell B} e^{-i\gamma_\ell C} \right) |\mathbf{s}\rangle, \quad |\mathbf{s}\rangle = |+\rangle^{\otimes n}. \quad (\text{B.1})$$

For an edge $e = (u, v)$ we consider

$$\langle \boldsymbol{\gamma}, \boldsymbol{\beta} | Z_u Z_v | \boldsymbol{\gamma}, \boldsymbol{\beta} \rangle = \langle \mathbf{s} | \left(\prod_{\ell=1}^p e^{i\gamma_\ell C} e^{i\beta_\ell B} \right) Z_u Z_v \left(\prod_{\ell=1}^p e^{-i\beta_\ell B} e^{-i\gamma_\ell C} \right) |\mathbf{s}\rangle. \quad (\text{B.2})$$

Complete-basis insertions in the Z basis. Insert $(2p+1)$ resolutions of identity in the Z -basis between neighboring operators and around $Z_u Z_v$. Using that C is diagonal in the Z -basis, $e^{\pm i\beta B} = \bigotimes_v e^{\pm i\beta X_v}$, and $\langle \mathbf{s} | \mathbf{z} \rangle = \langle \mathbf{z} | \mathbf{s} \rangle = 2^{-n/2}$, we have

$$\begin{aligned}
& \langle \boldsymbol{\gamma}, \boldsymbol{\beta} | Z_u Z_v | \boldsymbol{\gamma}, \boldsymbol{\beta} \rangle \\
&= \langle \mathbf{s} | e^{i\gamma_1 C} e^{i\beta_1 B} \dots e^{i\gamma_p C} e^{i\beta_p B} Z_u Z_v e^{i\gamma_{-p} C} e^{i\beta_{-p} B} \dots e^{-i\beta_1 B} e^{-i\gamma_1 C} | \mathbf{s} \rangle \\
&= \sum_{\{\mathbf{z}^{[i]}\}} \langle \mathbf{s} | \mathbf{z}^{[1]} \rangle e^{i\gamma_1 C(\mathbf{z}^{[1]})} \langle \mathbf{z}^{[1]} | e^{i\beta_1 B} \dots | \mathbf{z}^{[p]} \rangle e^{i\gamma_p C(\mathbf{z}^{[p]})} \langle \mathbf{z}^{[p]} | e^{i\beta_p B} | \mathbf{z}^{[0]} \rangle z_u^{[0]} z_v^{[0]} \\
&\quad \times \langle \mathbf{z}^{[0]} | \dots e^{-i\beta_2 B} | \mathbf{z}^{[-2]} \rangle e^{-i\gamma_2 C(\mathbf{z}^{[-2]})} \langle \mathbf{z}^{[-2]} | e^{-i\beta_1 B} | \mathbf{z}^{[-1]} \rangle e^{-i\gamma_1 C(\mathbf{z}^{[-1]})} \langle \mathbf{z}^{[-1]} | \mathbf{s} \rangle \quad (B.3) \\
&= \frac{1}{2^n} \sum_{\{\mathbf{z}^{[i]}\}} \exp \left[i\gamma_1 C(\mathbf{z}^{[1]}) + \dots + i\gamma_p C(\mathbf{z}^{[p]}) - i\gamma_p C(\mathbf{z}^{[-p]}) - \dots - i\gamma_1 C(\mathbf{z}^{[-1]}) \right] z_u^{[0]} \\
&\quad \times z_v^{[0]} \prod_{v=1}^n \langle z_v^{[1]} | e^{i\beta_1 X} | z_v^{[2]} \rangle \langle z_v^{[2]} | e^{i\beta_2 X} \dots | z_v^{[0]} \rangle \langle z_v^{[0]} | \dots e^{-i\beta_2 X} | z_v^{[-2]} \rangle \langle z_v^{[-2]} | e^{-i\beta_1 X} | z_v^{[-1]} \rangle.
\end{aligned}$$

Angle vector and one-site kernel. With

$$f(\mathbf{z}_v) = \frac{1}{2} \langle z_v^{[1]} | e^{i\beta_1 X} | z_v^{[2]} \rangle \dots \langle z_v^{[p]} | e^{i\beta_p X} | z_v^{[0]} \rangle \langle z_v^{[0]} | e^{-i\beta_p X} | z_v^{[-p]} \rangle \dots \langle z_v^{[-2]} | e^{-i\beta_1 X} | z_v^{[-1]} \rangle.$$

and

$$\boldsymbol{\Gamma} = \{\gamma_1, \dots, \gamma_p, 0, -\gamma_p, \dots, -\gamma_1\}$$

defined above, (B.2) becomes the vertex-factorized form

$$\langle \boldsymbol{\gamma}, \boldsymbol{\beta} | Z_u Z_v | \boldsymbol{\gamma}, \boldsymbol{\beta} \rangle = \frac{1}{2^n} \sum_{\{\mathbf{z}^{[j]}\}} \exp \left(i \sum_{j=-p}^p \Gamma_j C(\mathbf{z}^{[j]}) \right) (z_u^{[0]} z_v^{[0]}) \cdot \prod_{x \in V} f(\mathbf{z}_x). \quad (B.4)$$

p -locality and restriction to the lightcone. Let $H = G_p((u, v))$ be the p -local graph of the edge (u, v) as defined in Sec. 2.1, with vertex set $V(H) = N_p((u, v))$ and edge set given by (2.2). Since the Heisenberg-evolved observable for the edge $e = (u, v)$ is supported on $V(H)$, the phase term in (B.4) depends only on edges of H , and the mixer kernels factorize over $V \setminus V(H)$. Tracing out spins outside H therefore leaves

$$\langle \boldsymbol{\gamma}, \boldsymbol{\beta} | Z_u Z_v | \boldsymbol{\gamma}, \boldsymbol{\beta} \rangle = \sum_{\{\mathbf{z}_x : x \in V(H)\}} (z_u^{[0]} z_v^{[0]}) \exp \left(i \sum_{j=-p}^p \Gamma_j C_H(\mathbf{z}^{[j]}) \right) \prod_{x \in V(H)} f(\mathbf{z}_x), \quad (B.5)$$

where C_H is the unnormalized cut on H and $\mathbf{z}^{[j]}$ is restricted to $V(H)$. (B.5) is the localized master formula used by our dynamic programs.

C Lemmas and Proof Details

For completeness, we collect the proof sketches of several technical lemmas used in Sec. 3 (the presentation and notation are lightly normalized but the mathematical content is unchanged). Throughout, $Z_{x_0} Z_{y_0}$ denotes the two-qubit observable acting on endpoints (x_0, y_0) and $\text{MC} = \text{MAXCUT}(G')$.

C.1 Endpoint Consistency (Lemma 3.2)

Statement. For any vertex q , the dependence of the contribution to $\langle Z_u Z_v \rangle$ on $z_q^{[0]}$ falls into the following cases:

1. If $q \notin \{u, v\}$ and $z_q^{[p]} \neq z_q^{[-p]}$, then replacing $z_q^{[0]}$ by $-z_q^{[0]}$ flips the sign of the contribution. The two configurations related by this flip therefore cancel in the sum.
2. If $q \in \{u, v\}$ and $z_q^{[p]} = z_q^{[-p]}$, then flipping $z_q^{[0]}$ again flips the sign of the contribution, so the corresponding pair of configurations cancels.
3. In all remaining cases (that is, when $q \notin \{u, v\}$ with $z_q^{[p]} = z_q^{[-p]}$, or $q \in \{u, v\}$ with $z_q^{[p]} \neq z_q^{[-p]}$), the contribution is independent of $z_q^{[0]}$.

Proof. Denote by W the multiplicative factor from all spins and layers other than the two end-layer mixers acting on q (and, when $q \in \{u, v\}$, excluding the explicit observable factor $z_u^{[0]} z_v^{[0]}$). With $\beta_p = \frac{\pi}{4}$, the one-qubit mixer matrix elements in the Z -basis are

$$\langle a | e^{i\beta_p X} | b \rangle = \begin{cases} \cos\left(\frac{\pi}{4}\right) = \frac{1}{\sqrt{2}}, & a = b, \\ i \sin\left(\frac{\pi}{4}\right) = \frac{i}{\sqrt{2}}, & a = -b, \end{cases} \quad a, b \in \{\pm 1\}.$$

Case 1: $q \notin \{u, v\}$ and $z_q^{[p]} \neq z_q^{[-p]}$. Fix all other spins and compare the two configurations that differ only by $z_q^{[0]} = +1$ vs. -1 . The $z_q^{[0]}$ -dependent factor is the product of the two end-layer mixers on q . Writing the remaining (fixed) part as W , the two contributions are

$$W \cos\left(\frac{\pi}{4}\right) \left(\mp i \sin\left(\frac{\pi}{4}\right) \right), \quad (\text{C.1})$$

which are negatives of each other and sum to zero. This proves Item 1.

Case 2: $q \in \{u, v\}$ and $z_q^{[p]} = z_q^{[-p]}$. Here the observable contributes an extra factor $z_u^{[0]} z_v^{[0]}$, which flips sign when $z_q^{[0]}$ is flipped (exactly one endpoint bit changes). With the other-spin factor denoted by W , the two contributions for $z_q^{[0]} = \pm 1$ are

$$W \cos^2\left(\frac{\pi}{4}\right) \text{ and } -W \sin^2\left(\frac{\pi}{4}\right), \quad (\text{C.2})$$

when $z_q^{[p]} = z_q^{[-p]} = 1$ and

$$W - \cos^2\left(\frac{\pi}{4}\right) \text{ and } W \sin^2\left(\frac{\pi}{4}\right), \quad (\text{C.3})$$

when $z_q^{[p]} = z_q^{[-p]} = -1$. Again negatives of each other and hence cancel. This proves Item 2.

Case 3: Remaining two situations.

(3a) $q \notin \{u, v\}$ with $z_q^{[p]} = z_q^{[-p]}$. For any valid configuration with contribution W , flipping $z_q^{[0]}$ changes the mixer product on q from $\cos^2\left(\frac{\pi}{4}\right)$ to $-(i \sin\left(\frac{\pi}{4}\right))^2 = \sin^2\left(\frac{\pi}{4}\right)$ or vice versa. Thus the new contribution equals

$$W \cdot \frac{-i^2 \sin^2\left(\frac{\pi}{4}\right)}{\cos^2\left(\frac{\pi}{4}\right)} = W, \quad (\text{C.4})$$

or, symmetrically,

$$W \cdot \frac{\cos^2\left(\frac{\pi}{4}\right)}{-i^2 \sin^2\left(\frac{\pi}{4}\right)} = W, \quad (\text{C.5})$$

so the value is independent of $z_q^{[0]}$.

(3b) $q \in \{u, v\}$ with $z_q^{[p]} \neq z_q^{[-p]}$. Let the original contribution be W . When $(z_q^{[p]}, z_q^{[0]}, z_q^{[-p]}) = (1, 1, -1)$ or $(1, -1, -1)$, flipping $z_q^{[0]}$ gives

$$W \cdot \frac{-i \sin\left(\frac{\pi}{4}\right) \cos\left(\frac{\pi}{4}\right)}{-i \sin\left(\frac{\pi}{4}\right) \cos\left(\frac{\pi}{4}\right)} = W, \quad (\text{C.6})$$

and when $(z_q^{[p]}, z_q^{[0]}, z_q^{[-p]}) = (-1, -1, 1)$ or $(-1, 1, 1)$, flipping $z_q^{[0]}$ gives

$$W \cdot \frac{i \sin(\frac{\pi}{4}) \cos(\frac{\pi}{4})}{i \sin(\frac{\pi}{4}) \cos(\frac{\pi}{4})} = W. \quad (\text{C.7})$$

In both subcases the contribution is unchanged, hence independent of $z_q^{[0]}$.

Combining the three cases establishes the claim. \square

C.2 Asynchronous Flips (Lemma 3.3)

Statement. For the observable $Z_{x_0}Z_{y_0}$, if $z_{x_0}^{[p]} \neq z_{y_0}^{[p]}$, then there is no contribution to coefficients with exponents

$$k \geq \left((p-1) \text{MC} + 200n_0^2 + 2n_0(11n_0 + 1) \right).$$

Proof. Fix a configuration $\{\mathbf{z}\} = (z_v^{[j]})_{v \in V(G'), j = -p, \dots, p}$ with $z_{x_0}^{[p]} \neq z_{y_0}^{[p]}$. As in Eq. (3.3), the exponent contributed by $\{\mathbf{z}\}$ is

$$D(\mathbf{z}) = \sum_{j=1}^p (C_j(\mathbf{z}) - C_{-j}(\mathbf{z})),$$

where $C_j(\mathbf{z})$ denotes the cut value of G' on layer j . Since every $C_j(\mathbf{z})$ is a cut of G' , we have $0 \leq C_j(\mathbf{z}) \leq \text{MC}$ for all j , where $\text{MC} = \text{MAXCUT}(G')$. In particular, for the inner layers $j = 1, \dots, p-1$ we obtain

$$C_j(\mathbf{z}) - C_{-j}(\mathbf{z}) \leq \text{MC},$$

and hence

$$D(\mathbf{z}) = \sum_{j=1}^{p-1} (C_j(\mathbf{z}) - C_{-j}(\mathbf{z})) + (C_p(\mathbf{z}) - C_{-p}(\mathbf{z})) \leq (p-1) \text{MC} + (C_p(\mathbf{z}) - C_{-p}(\mathbf{z})).$$

Therefore, to show that no configuration with $z_{x_0}^{[p]} \neq z_{y_0}^{[p]}$ can contribute to a coefficient with exponent

$$k \geq (p-1) \text{MC} + 200n_0^2 + 2n_0(11n_0 + 1),$$

it suffices to prove that, under this hypothesis,

$$C_p(\mathbf{z}) - C_{-p}(\mathbf{z}) < 200n_0^2 + 2n_0(11n_0 + 1). \quad (\text{C.8})$$

We now analyze $C_p(\mathbf{z}) - C_{-p}(\mathbf{z})$ by exploiting endpoint consistency (Lemma 3.2). Recall that for any vertex $q \notin \{x_0, y_0\}$, if $z_q^{[p]} \neq z_q^{[-p]}$, then flipping $z_q^{[0]}$ reverses the sign of the contribution of $\{\mathbf{z}\}$ without changing the exponent. Thus, in the coefficient of any fixed Laurent exponent, all such configurations cancel pairwise. Consequently, when bounding (C.8) for nonvanishing coefficients, we may restrict attention to configurations obeying

$$z_q^{[p]} = z_q^{[-p]} \quad \text{for all } q \notin \{x_0, y_0\}. \quad (\text{C.9})$$

Applying Lemma 3.2 with $q \in \{x_0, y_0\}$ shows that, in order to avoid cancellation, we must have $z_{x_0}^{[p]} \neq z_{x_0}^{[-p]}$ and $z_{y_0}^{[p]} \neq z_{y_0}^{[-p]}$; otherwise flipping the corresponding layer-0 spin would again flip the sign of the contribution and force cancellation. Since we are in the case $z_{x_0}^{[p]} \neq z_{y_0}^{[p]}$, we have $z_{x_0}^{[p]} z_{y_0}^{[p]} = -1$. Multiplying the two inequalities $z_{x_0}^{[p]} \neq z_{x_0}^{[-p]}$ and $z_{y_0}^{[p]} \neq z_{y_0}^{[-p]}$ yields

$$z_{x_0}^{[p]} z_{x_0}^{[-p]} = -1, \quad z_{y_0}^{[p]} z_{y_0}^{[-p]} = -1,$$

so

$$(z_{x_0}^{[p]} z_{y_0}^{[p]})(z_{x_0}^{[-p]} z_{y_0}^{[-p]}) = 1,$$

and hence also $z_{x_0}^{[-p]} \neq z_{y_0}^{[-p]}$. In particular, the spins at x_0 and y_0 are opposite on both boundary layers $\pm p$.

Recall that

$$C_j(\mathbf{z}) = \sum_{(u,v) \in E(G')} \frac{1}{2} (1 - z_u^{[j]} z_v^{[j]}),$$

so the difference $C_p(\mathbf{z}) - C_{-p}(\mathbf{z})$ receives a nonzero contribution from an edge (u, v) only if its cut/non-cut status differs between layers p and $-p$. We now consider edges by their relation to $\{x_0, y_0\}$.

Edges not incident to x_0 or y_0 . For such an edge (u, v) both endpoints satisfy (C.9), so $z_u^{[p]} = z_u^{[-p]}$ and $z_v^{[p]} = z_v^{[-p]}$. Therefore the product $z_u^{[j]} z_v^{[j]}$ is identical for $j = p$ and $j = -p$, and the edge contributes equally to $C_p(\mathbf{z})$ and $C_{-p}(\mathbf{z})$. Hence these edges contribute zero to $C_p(\mathbf{z}) - C_{-p}(\mathbf{z})$.

Edges between $\{x_0, y_0\}$ and $V(G') \setminus (X \cup Y \cup \{x_0, y_0\})$. By construction of G' , every vertex outside the global bipartite frame $X \cup Y$ that is adjacent to x_0 or y_0 is in fact adjacent to *both* x_0 and y_0 (these are the vertices in the blow-up gadgets $B(u)$ for $u \in V(G)$, together with the controller w). Let u be such a vertex. Then (C.9) gives $z_u^{[p]} = z_u^{[-p]}$, while the previous paragraph shows that $z_{x_0}^{[-p]} = -z_{x_0}^{[p]}$ and $z_{y_0}^{[-p]} = -z_{y_0}^{[p]}$. Writing $s = z_u^{[p]}$ and choosing signs so that $z_{x_0}^{[p]} = +1$, $z_{y_0}^{[p]} = -1$, we have

$$\begin{aligned} \frac{1}{2}(1 - z_u^{[p]} z_{x_0}^{[p]}) + \frac{1}{2}(1 - z_u^{[p]} z_{y_0}^{[p]}) &= \frac{1}{2}(1 - s) + \frac{1}{2}(1 + s) = 1, \\ \frac{1}{2}(1 - z_u^{[-p]} z_{x_0}^{[-p]}) + \frac{1}{2}(1 - z_u^{[-p]} z_{y_0}^{[-p]}) &= \frac{1}{2}(1 + s) + \frac{1}{2}(1 - s) = 1. \end{aligned}$$

Thus the *pair* of edges (u, x_0) and (u, y_0) contributes the same total amount to $C_p(\mathbf{z})$ and to $C_{-p}(\mathbf{z})$, and hence contributes zero to their difference. Summing over all such vertices u , we conclude that edges between $\{x_0, y_0\}$ and $V(G') \setminus (X \cup Y \cup \{x_0, y_0\})$ do not affect $C_p(\mathbf{z}) - C_{-p}(\mathbf{z})$.

Edges within the global frame $X \cup Y$. We are left with edges whose endpoints lie in the bipartite frame. Among these, the special edge (x_0, y_0) has endpoints that are opposite on both layers p and $-p$, so it is cut on both layers and contributes equally to $C_p(\mathbf{z})$ and $C_{-p}(\mathbf{z})$; hence its contribution to the difference again vanishes.

All remaining edges incident to x_0 or y_0 have the form (x_0, y) with $y \in Y \setminus \{y_0\}$ or (x, y_0) with $x \in X \setminus \{x_0\}$. There are exactly

$$(|Y| - 1) + (|X| - 1) = (100n_0^2 - 1) + (100n_0^2 - 1) = 200n_0^2 - 2$$

such edges. For each of these edges, the neighbor in $X \cup Y$ has the same spin on layers p and $-p$, while x_0 or y_0 flips between the two layers. Thus, in the most favorable situation for maximizing $C_p(\mathbf{z}) - C_{-p}(\mathbf{z})$, we may assume that every such edge is cut at layer p and uncut at layer $-p$, contributing 1 to the difference. Therefore,

$$C_p(\mathbf{z}) - C_{-p}(\mathbf{z}) \leq 200n_0^2 - 2.$$

This immediately implies

$$C_p(\mathbf{z}) - C_{-p}(\mathbf{z}) \leq 200n_0^2 - 2 < 200n_0^2 + 2n_0(11n_0 + 1),$$

which is exactly (C.8). Combining this with the earlier bound $D(\mathbf{z}) \leq (p - 1) \text{MC} + (C_p(\mathbf{z}) - C_{-p}(\mathbf{z}))$, we obtain

$$D(\mathbf{z}) < (p - 1) \text{MC} + 200n_0^2 + 2n_0(11n_0 + 1)$$

for every configuration with $z_{x_0}^{[p]} \neq z_{y_0}^{[p]}$ that survives the cancellations enforced by Lemma 3.2. Hence no such configuration can contribute to coefficients with exponent $k \geq (p - 1) \text{MC} + 200n_0^2 + 2n_0(11n_0 + 1)$, as claimed. \square

C.3 Attainability of the Largest Nonzero Exponent (Lemma 3.4)

Statement. For the observable $Z_{x_0}Z_{y_0}$, the largest nonzero exponent in $h_{(x_0, y_0)}$ attainable by the induced polynomial is

$$\left((p-1) \text{MC} + 200n_0^2 + 2n_0(11n_0 + 1) \right). \quad (\text{C.10})$$

We prove two parts: (i) *Maximality*: the upper bound of the exponent in the display above is attainable; (ii) *Non-vanishing*: the coefficient of the term at that exponent is nonzero.

Notation. For any configuration $\{\mathbf{z}\}$, denote its monomial contribution to the exponent term by

$$\text{Contr}(\mathbf{z}) := f(\mathbf{z}) z_{x_0}^{[0]} z_{y_0}^{[0]},$$

and the corresponding exponent by

$$D(\mathbf{z}) := \sum_{j=1}^p (C_j(\mathbf{z}) - C_{-j}(\mathbf{z})),$$

where $C_j(\mathbf{z})$ and $C_{-j}(\mathbf{z})$ are the cut values on layers j and $-j$, respectively. Let MC be a uniform upper bound for the inner-layer difference.

Maximality *Goal and idea.* If each difference $C_j(\mathbf{z}) - C_{-j}(\mathbf{z})$ can simultaneously attain its individual upper bound, then their sum $\sum_{j=1}^p (C_j(\mathbf{z}) - C_{-j}(\mathbf{z}))$ is naturally maximized.

1. *Inner layers* ($1 \leq j \leq p-1$) *fixed at extremum.* For $j \in [1, p-1]$, take $C_j(\mathbf{z}) - C_{-j}(\mathbf{z}) = \text{MC}$, so that the inner-layer contribution is exactly $(p-1) \text{MC}$.
2. *Necessary constraints and non-vanishing on the end layers* ($j = \pm p$). To avoid cancellation on the end layers and to ensure a nonzero coefficient, Lemmas 3.2 and 3.3 allow us to restrict feasible configurations to those satisfying the following necessary conditions (“endpoint consistency / asynchronous flips yield no large exponent”):

- (i) $\forall u \notin \{x_0, y_0\} : z_u^{[p]} = z_u^{[-p]}$;
- (ii) $\forall u \in \{x_0, y_0\} : z_u^{[p]} \neq z_u^{[-p]}$;
- (iii) $z_{x_0}^{[p]} = z_{y_0}^{[p]}$.

Moreover, to maximize $C_p(\mathbf{z}) - C_{-p}(\mathbf{z})$ we impose:

- (iv) All non-endpoint spins on layer p are identical and opposite to $z_{x_0}^{[p]} = z_{y_0}^{[p]}$.

3. *Achievable upper bound for the end-layer maximum difference.* Under (i)–(iv), the entire effective contribution from the end layers is generated by flipping x, y from p to $-p$; via explicit construction and an upper-bound estimate we have

$$\begin{aligned} \max(C_p(\mathbf{z}) - C_{-p}(\mathbf{z})) &= \max_{(u,v) \in E} (d(u) + d(v) - 2) \\ &= d(x_0) + d(y_0) - 2 \\ &= 200n_0^2 + 2n_0(11n_0 + 1) \end{aligned}$$

Here, “attainability” follows from the explicit arrangement of endpoints and non-endpoints given in the main text; the “upper bound” follows from the maximum gain accrued by the number of edges adjacent to x_0, y_0 when they flip between the two end layers, subtracting the amplifier edge between (x_0, y_0) to obtain the net value.

In summary, the inner layers contribute $(p-1) \text{MC}$ and the end layers contribute $200n_0^2 + 2n_0(11n_0 + 1)$. Therefore the attainable upper bound of the largest exponent is

$$(p-1) \text{MC} + 200n_0^2 + 2n_0(11n_0 + 1),$$

namely as in (3.7).

Non-vanishing We prove that the coefficient of the term at the exponent

$$D_{\max} = \left((p-1) \text{MC} + 200n_0^2 + 2n_0(11n_0 + 1) \right)$$

is *nonzero*.

Configurations achieving the largest exponent: necessary and sufficient conditions We first characterize the family of configurations that can reach the largest exponent D_{\max} . The following conditions are *necessary and sufficient*:

- (1) For $i \in [1, p-1]$, take $C_i(\mathbf{z}) = \text{MC}$; for $i \in [-p, -1]$, take $C_i(\mathbf{z}) = 0$.
- (2) On the end layers, $z_{x_0}^{[p]} = z_{y_0}^{[p]} \neq z_{x_0}^{[-p]} = z_{y_0}^{[-p]}$.
- (3) For all $u \in V \setminus \{x_0, y_0\}$, $z_u^{[p]} = z_u^{[-p]}$.
- (4) All non-endpoint spins on layer p are identical and *opposite* to $z_{x_0}^{[p]} = z_{y_0}^{[p]}$.

Explanation of necessity and sufficiency. If any one of the above fails, the differences $C_j(\mathbf{z}) - C_{-j}(\mathbf{z})$ for all $j \in [1, p]$ cannot jointly attain their upper bounds; conversely, if (1)–(4) hold, then each layer difference can be maximized, thereby achieving the largest exponent D_{\max} .

Ignoring configurations containing a $\sin \psi$ factor If there exist $u \in V$ and some $i \in [1, p-1] \cup [-p+1, -1]$ such that $z_u^{[i]} \neq z_u^{[i+1]}$, then the amplitude of that configuration contains at least one factor $\sin \psi = 2^{O(-n^2)}$, and its contribution is dominated by configurations without $\sin \psi$. Hence such configurations can be ignored (this does not affect the final non-vanishing conclusion, Because even if there are $2^{O(n)}$ such terms, the sum of their moduli is smaller than the modulus of a single term without the $\sin \psi$ factor; see also below that their sum is nonzero).

Fixing the value of w : equal amplitude and end-layer structure For convenience, first *fix* the configuration of the controller w . Under (1)–(4), only these configurations can reach the largest exponent. We show that the monomial contributions of these configurations have *equal value*.

- *Uniform value of inner-layer transitions:*

- (i) For $u \in V$ and $i \in [1, p-1] \cup [-p+1, -1]$, $\langle z_u^{[i]} | e^{i\beta_i X} | z_u^{[i+1]} \rangle = \cos \psi$.
- (ii) For $i \in V$ and $i = -p$, $\langle z_u^{[i]} | e^{i\beta_i X} | z_u^{[i+1]} \rangle = \cos \frac{\pi}{4}$.
- (iii) For the forward boundary layer $i = p-1$, we use the Max-Cut structure. Fix the spin of w , and consider only configurations that attain the largest exponent. By construction of the reduction, these configurations correspond to maximum cuts $(S, V \setminus S)$ of G' satisfying:

- x_0 and y_0 lie on opposite sides of the cut;
- we may assume $w \in V \setminus S$;
- each such maximum cut of G' induces a maximum cut of the original instance G , and we refine our choice so that the induced cut on G maximizes $|S \cap V(G)|$.

With this tie-breaking, once the spin of w is fixed, the number of vertices $u \in V(G)$ that lie in S is the same for every configuration achieving the largest exponent. Equivalently, the number of vertices u for which $z_u^{[p-1]} \neq z_u^{[p]}$ is *independent* of the particular maximizing configuration. At the boundary choice $\beta_{p-1} = \frac{\pi}{4}$, each one-qubit factor $\langle z_u^{[p-1]} | e^{i\beta_{p-1} X} | z_u^{[p]} \rangle$

has value $\cos \frac{\pi}{4}$ when $z_u^{[p-1]} = z_u^{[p]}$ and value $i \sin \frac{\pi}{4}$ when $z_u^{[p-1]} \neq z_u^{[p]}$, and the number of “flip” transitions is fixed across all maximizers. Therefore the product

$$\prod_{u \in V'} \langle z_u^{[p-1]} | e^{i\beta_{p-1} X} | z_u^{[p]} \rangle$$

has the same value for all configurations that achieve the largest exponent. Hence, within the family of configurations that can reach the largest exponent, the inner-layer contribution is identical.

- *Uniform value across the three end layers $(p, 0, -p)$:*

(i) For any $u \in V \setminus \{x_0, y_0\}$, the product $\langle z_u^{[p]} | e^{i\beta_p X} | z_u^{[0]} \rangle \langle z_u^{[0]} | e^{-i\beta_p X} | z_u^{[-p]} \rangle$ takes the *same* value across all configurations achieving the largest exponent;
(ii) The endpoint factor $z_{x_0}^{[0]} z_{y_0}^{[0]} \prod_{u \in \{x_0, y_0\}} \langle z_u^{[p]} | e^{i\beta_p X} | z_u^{[0]} \rangle \langle z_u^{[0]} | e^{-i\beta_p X} | z_u^{[-p]} \rangle$ is also *identical*.

It follows that, with w fixed, the configurations achieving the largest exponent have *equal contributions*. Moreover, the sum of contributions corresponding to the two choices of w is also the same; this will be used together with the “places where w may vary” in the next step.

The only two places that change w and the four types of contributions Consider when the value of w *changes*. Clearly, only two places can change the spin of w :

$$(z_w^{[p-1]}, z_w^{[p]}) \quad \text{and} \quad (z_w^{[-p]}, z_w^{[-p+1]}).$$

Under the properties of configurations that can reach the largest exponent:

- The first change swaps the “bits that should flip” with those that should not, thereby flipping $n - r$ bits and introducing a factor i^{n-r} (where r is the number of bits that should flip).
- The second change flips *all* vertices, multiplying the contribution by $(-i)^n$.

Accordingly, classifying by whether w is changed at these two places, the four representative contributions are

$$\begin{array}{ll} (\text{unchanged, unchanged}) : & i^r T, \\ & (\text{unchanged, changed}) : -i^{r+n} T, \\ (\text{changed, unchanged}) : & i^{n-r} T, \\ & (\text{changed, changed}) : -i^{2n-r} T, \end{array}$$

where $T > 0$ is a common real magnitude, and r is the maximum, over all maximum-cut assignments, of the number of vertices whose configuration differs from that of w . To compare their *phase sum*, multiply all four terms by $T^{-1}i^{3r}$ to obtain

$$1, \quad -i^n, \quad i^{n+2r}, \quad -i^{2n+2r}.$$

We then distinguish cases by the parity of r and of n (in our construction, $n = 211n_0^2 + n_0 + 1$ is odd):

- *r odd*: The four terms are $1, -i^n, i^{n+2r}, -1$. Using $i^{n+2r} = -i^n$,

$$1 - 1 - i^n - i^n = -2i^n \neq 0,$$

hence the phase sum is nonzero.

- *r even*: The four terms are $1, -i^n, i^n, -i^{2n}$. Since $i^{2n} = (-1)^n$,

$$1 - (-1)^n + i^n - i^n = 1 - (-1)^n = 2 \neq 0,$$

so the phase sum is again nonzero.

Conclusion Within the family of configurations achieving the largest exponent D_{max} , each single contribution has *equal magnitude*; the *sum of phases* over the four representative configurations above is *nonzero*. Therefore the coefficient of the Laurent term at exponent D is *nonzero*, proving “non-vanishing.”

Combining “maximality” and “non-vanishing” shows that the exponent in (3.7) is both attainable and has a nonzero coefficient, so $D_{max} = ((p-1)MC + 200n_0^2 + 2n_0(11n_0 + 1))$ is the **largest nonzero exponent** for $Z_{x_0}Z_{y_0}$, completing the proof of Lemma 3.4. \square

C.4 Upper Bound for Other Edges (Lemma 3.5)

Statement. Let the observable be Z_iZ_j with $(i, j) \notin \{(x_0, y_0), (y_0, x_0)\}$. Then all coefficients of the terms in $h_{(i,j)}$ with exponents $\geq ((p-1)MC + 200n_0^2 + 2n_0(11n_0 + 1))$ vanish.

Proof. First suppose exactly one endpoint is in $\{x_0, y_0\}$, say the observable is $Z_{x_0}Z_o$ for some $o \in V(G') \setminus \{y_0\}$. Because $\sum_{i=1}^{p-1} (C_i(\mathbf{z}) - C_{-i}(\mathbf{z})) \leq (p-1)MC$ and Lemma 3.2, we have

$$\begin{aligned} C_p(\mathbf{z}) - C_{-p}(\mathbf{z}) &\leq d(x_0) + d(o) - 2 \\ &\leq n_0(11n_0 + 1) + 1 + 100n_0^2 + 100n_0^2 - 2 \\ &< d(x_0) + d(y_0) - 2 \end{aligned}$$

which is at most the degrees of the two endpoints. So

$$\sum_{i=1}^p (C_i(\mathbf{z}) - C_{-i}(\mathbf{z})) < ((p-1)MC + 200n_0^2 + 2n_0(11n_0 + 1)).$$

which means that the term of the highest non-zero degree in the polynomial $h_{(x_0,o)}(x)$, obtained by taking edges with exactly one of (x_0, y_0) as an endpoint as observables, is less than D_{max} .

If neither endpoint is in $\{x_0, y_0\}$, then

$$\sum_{i=1}^{p-1} (C_i(\mathbf{z}) - C_{-i}(\mathbf{z})) \leq (p-1)MC \tag{C.11}$$

and

$$C_p(\mathbf{z}) - C_{-p}(\mathbf{z}) < d(i) + d(j) \leq 200n_0^2. \tag{C.12}$$

Thus the largest exponent attainable is at most $((p-1)MC + 200n_0^2)$ which is less than D_{max} proving the claim. \square

C.5 Magnitude of the Extreme-Term Coefficients (Lemma 3.6)

Statement. Let D_{max} be the maximal exponent that appears with nonzero coefficients in the Laurent polynomial $h_{(x_0,y_0)}(x)$ induced by the observable $Z_{x_0}Z_{y_0}$ (cf. Sec. 3). Then

$$|w(D_{max})| \geq 2^{-2n-1}.$$

Proof. Fix the canonical family of configurations from Lemma 3.4 that attain D_{max} in (3.7): layers $j = 1, \dots, p-1$ take a common maximum cut; layers $j = -1, \dots, -(p-1)$ take a common minimum cut; and the boundary layers $\{\pm p, 0\}$ are set as in that construction. For any such configuration, the absolute magnitude of its contribution factorizes into (i) the two overlaps with $|s\rangle = |+\rangle^{\otimes n}$ and (ii) on-site one-qubit transition amplitudes coming from the mixers:

(a) *Overlaps with $|s\rangle$.* From the complete-basis insertions, the two overlaps contribute a uniform factor 2^{-n} .

(b) $\frac{\pi}{4}$ mixers at the outer boundary $\pm p$. With $\beta_p = \frac{\pi}{4}$, for each qubit and for each of the two boundary mixers the one-qubit transition amplitude has magnitude in $\{\cos(\frac{\pi}{4}), \sin(\frac{\pi}{4})\} = 2^{-1/2}$. Hence the total outer-boundary mixer magnitude is 2^{-n} .

(b') $\frac{\pi}{4}$ mixers at the near-boundary transitions $p - 1 \rightarrow p$ and $-p \rightarrow -p + 1$. Under the parameter choice $\beta_{p-1} = \frac{\pi}{4}$, these two additional near-boundary mixer blocks contribute another factor 2^{-n} in magnitude across n qubits.

(c) *Inner mixers.* Excluding the four $\frac{\pi}{4}$ boundary/near-boundary mixer blocks $\{\pm p, p - 1, -p + 1\}$, each qubit undergoes exactly $2(p - 2)$ inner mixer transitions, each contributing a factor $\cos \psi$, where the parameter choice in Sec. 3 ensures $\cos \psi \geq 1 - 2^{-n^2}$. Therefore, across all qubits,

$$(\cos \psi)^{2n(p-2)} \geq (1 - 2^{-n^2})^{2n(p-2)} \geq 1 - 2n(p-2) \cdot 2^{-n^2} \geq \frac{3}{4}$$

for all sufficiently large n (Bernoulli's inequality and $p \geq 2$).

Multiplying (a), (b), (b'), and (c), each fixed configuration contributes at least $2^{-n} \cdot 2^{-n} \cdot 2^{-n} \cdot \frac{3}{4} = 3 * 2^{-3n-2}$ in absolute value. By Endpoint Consistency (Lemma 3.2) together with the $\frac{\pi}{4}$ phase-pairing argument, the integrand is insensitive to the entire layer-0 string; hence summing over this layer multiplies the contribution by 2^n . Note that the terms with the $\sin \psi$ factor are equivalent to a small perturbation $\delta \leq 2^{O(n)} * 2^{O(-n^2)} = 2^{O(-n^2)}$ here. Thus

$$|w(D_{\max})| \geq 2^n \cdot \frac{3}{4} \cdot 2^{-3n} - \delta \geq 2^{-2n-1}.$$

□